2018

The Characterization of a Novel Complex Implicated in the Initiation of Apoptosis

Thomas Hsiao

THE CHARACTERIZATION OF A NOVEL COMPLEX IMPLICATED IN THE INITIATION OF APOPTOSIS

A Thesis Presented to the Faculty of

The Rockefeller University

in Partial Fulfillment of the Requirements for

the degree of Doctor of Philosophy

by

Thomas Hsiao

June 2018

THE CHARACTERIZATION OF A NOVEL COMPLEX IMPLICATED IN THE INITIATION OF APOPTOSIS

Thomas Hsiao, Ph.D.

The Rockefeller University 2018

Apoptosis, which is one of many different types of programmed cell death, is widely utilized as a mechanism to eliminate unwanted cells. The ability of cells to undergo apoptosis is required not only for development in many organisms, but also to maintain proper homeostasis; too little apoptosis can result in cancer whereas too much can lead to degenerative diseases. Apoptosis has been well studied at events that take place at or downstream of the mitochondria; these steps are rigorous and predictable, making them easy to study. However, little is known about early, decision-making events that occur upstream of the mitochondria. It is important to understand these early decision-making steps because it is at these timepoints when cells are not yet committed to live or die, and therefore have great potential for therapeutic intervention.

We have identified a novel ARTS-dependent complex that forms extremely early in apoptosis. After inducing mammalian cells to die, we fractionated the cell extracts using gel filtration and looked for changes in canonical apoptosis proteins. We observed that XIAP, the main caspase inhibitor in mammals, is recruited to a 5Mda complex as early as 30 minutes after stimulation of apoptosis. Furthermore, the recruitment of XIAP to the complex is dependent on the pro-apoptotic protein ARTS, as XIAP is not recruited to the complex when cells are knocked out for ARTS.

Using mass spectrometry, we have identified the constituents of the complex. The identified subunits are Herc2, Neurl4, SSSCA1 and XIAP. None of the identified subunits, aside from

XIAP, have been previously implicated in apoptosis. Using cell culture assays, we have shown that the novel complex acts to degrade XIAP, thus shifting the propensity of cells to undergo apoptosis early on in the decision-making process. We have shown that knocking down Neurl4 leads to the stabilization of XIAP during apoptosis and, consequently, reduces the number of cells that undergo apoptosis. The identification and elucidation of this novel complex in apoptosis not only increases our basic understanding of apoptosis, but also provides new therapeutic opportunities for modulating cell death.

ACKNOWLEDGEMENTS

I would first like to extend my gratitude to my mentor, Hermann Steller. It has truly been a privilege to have Hermann as an advisor. One cannot help but be inspired by Hermann's understanding and insight about science. However, what impresses me the most is Hermann's compassion and understanding beyond science. Time and time again, Hermann has shown that he appreciates and understands the human aspects and tribulations that accompany a career in science. Not only is he a great scientific advisor, but also a wonderful friend. As a result, Hermann has been able to create a lab composed of people who are not only great scientists, but are also a joy to be around; it has been a pleasure to do my thesis work in such a great environment.

I am also grateful to my esteemed committee: Shai Shaham, the late Günter Blobel, Elias Coutavas for serving in the place of Günter and my external committee member Hyung Don Ryoo. I would also like to thank Sarit Larisch for her support, unwavering enthusiasm and collaboration throughout the entirety of my project. Having such great committee members and advisors has kept me inspired and on track during this rollercoaster of a journey.

Finally, I would like to acknowledge those closest to me who have made this journey possible. I thank my family, who have always shown me unconditional love and support. In particular, I want to thank my mother, Gale Summerfield, whose pursuit of knowledge and kindness toward others has always given me something to strive for. And I would like to thank my friends, Rene Adam, Sean Woodward, Zeeshan Ozair, Ali Cihan, Sandra Jones, Joe Rodriguez, John Hays, Kai Liu, Yetis Gultekan, and Dana Mamriev. I am extremely grateful for having such wonderful friends who are always willing to listen, whether it be about science or life.

TABLE OF CONTENTS

LIST OF FIGURES

CHAPTER 1: INTRODUCTION

We live in a dynamic world where life is constantly being challenged and requires continuous adaptation. Consequently, organisms have evolved myriad ways to respond to an ever-changing environment. A process fundamental for proper fitness in higher organisms is apoptosis, which is a type of programmed cell death that is utilized throughout life, from development to coping with stresses. The precise and faithful regulation of apoptosis is paramount; too much apoptosis can result in degenerative diseases whereas too little can result in autoimmune diseases and cancer. Our understanding of apoptosis has come a long way since it was first observed in 1842, and as we continue to learn about it, we will be presented with new therapeutic opportunities to better treat many diseases.

Apoptosis is an active process characterized by distinct morphological changes, such as cell shrinkage, chromatin condensation, retained membrane integrity and inversion of the cell membrane (Jacobson, Weil, & Raff, 1997). These changes are not seen in passive cell death, termed necrosis, which results in the cell swelling and ultimately rupturing. Apoptosis is used to eliminate cells which have received stimuli to die, such as extensive DNA damage, viral infection or hormonal signals. The current consensus is that the regulation of apoptosis largely takes place at the mitochondria, where pro-apoptotic proteins are being continuously inhibited by anti-apoptotic proteins. Once pro-apoptotic proteins overwhelm their anti-apoptotic counterparts, the mitochondria undergo mitochondrial outer membrane permeabilization (MOMP), releasing several pro-apoptotic factors such as cytochrome C, a so-called point of no return where cells are now committed to die (Figure 1.1).

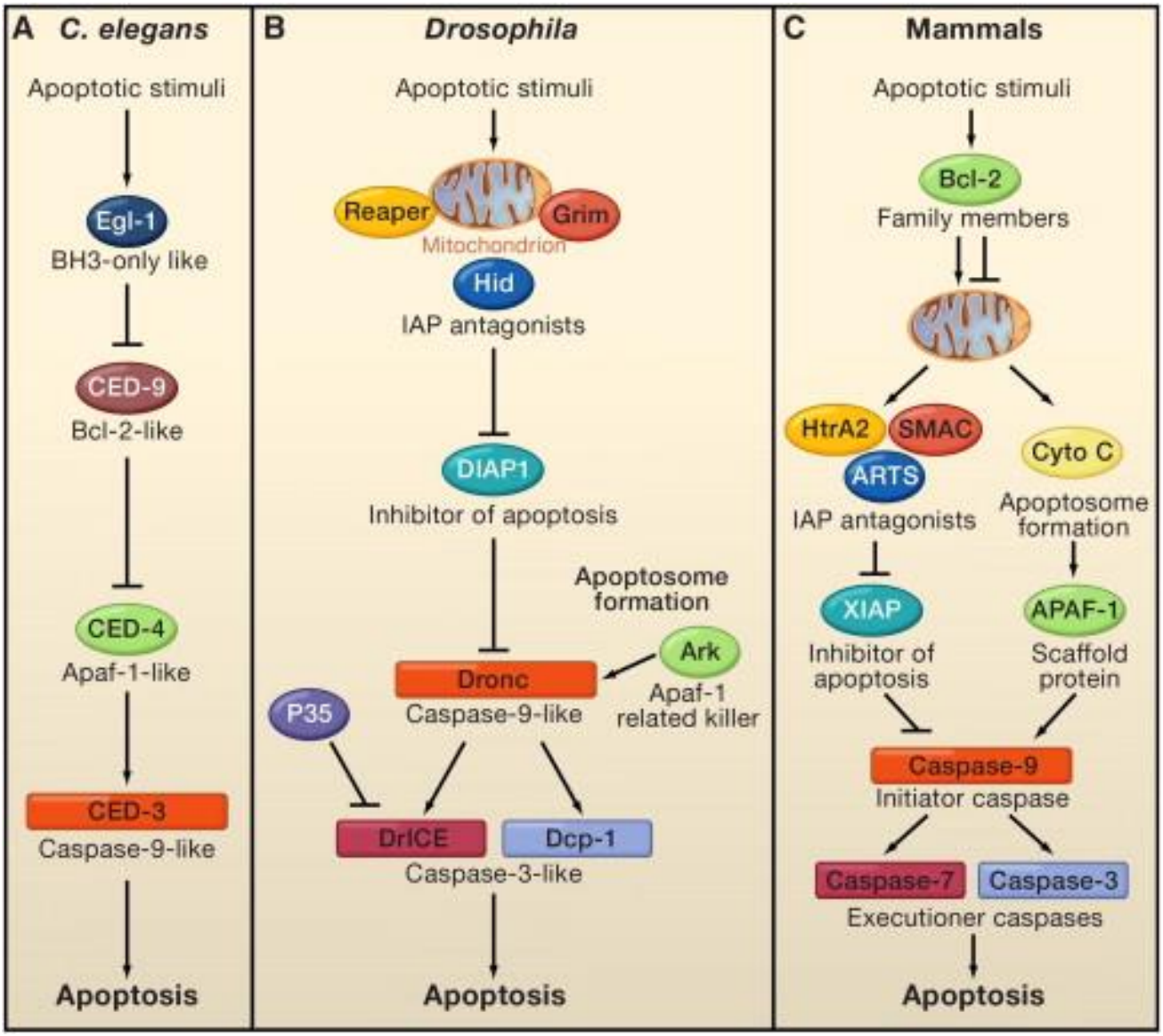

Figure 1.1: The core apoptotic pathway in C. elegans, Drosophila Melanogaster and Mammals. Apoptosis has been extensively studied in many organisms. However, most of what we know about apoptosis occurs either at or downstream of the mitochondria. The aim of this thesis is to understand events that take place during the decision-making phase of apoptosis, which is upstream of mitochondria permeabilization (Fuchs & Steller, 2011).

One of the most upstream events of apoptosis is the sensing of cellular damage. The protein p53 is a well-studied regulator of apoptosis that is known to detect intracellular damage. When p53 is activated, it translocates to the nucleus, where it activates the transcription of pro-apoptotic genes NOXA and PUMA (Oda, 2000; Nakano, 2001). The expression of Puma and Noxa induces

MOMP by activating Bax/Bak, which are pro-apoptotic Bcl-2 family members that form pores in the outer mitochondrial membrane (Oltvai, 1993; Farrow, 1995). MOMP then results in the release of pro-apoptotic mitochondrial factors into the cytosol, such as Smac/Diablo, Omi/HtrA2, AIF and cytochrome C (Du, 2000; Joza, 2001; Martins, 2001; Verhagen, 2000; Zou, 1997).

After cytochrome C is released into the cytosol, it binds to Apaf1, causing its oligomerization and recruitment of Caspase-9 (Rodriguez, 1999; Xuan, 1992; Zou, 1997). The resulting complex is termed the apoptosome and its function is to activate Caspase-9 (Seshagiri, 1997). After Caspase-9 is activated, it is able to activate Caspase-3 by removing its pro-domain (Fernandes-Alnemri, 1994; Nicholson, 1995). The activation of caspases is a critical step in inducing apoptosis.

Caspases are cysteine proteases that are central downstream components of the apoptotic machinery. They contain inhibitory pro-domains and are activated when the pro-domain is cleaved off. Initiator caspases include Caspase-8 and 9 and are responsible for the activation of executioner caspases. Executioner caspases include caspases 3 and 7 and once activated, go on to cleave numerous substrates responsible for the apoptotic phenotype. Therefore, the tight regulation of caspases is critical in preventing aberrant cell death.

Inhibitors of apoptosis (IAPs), as their name suggests, are an important class of proteins for putting the brakes on cell death. IAPs are able to directly bind caspases via their BIR domains. XIAP, which has been extensively studied among the IAPs, can inhibit initiator Caspase-9 as well as executioner Caspases 3 and 7, and serves as a threshold that must be overcome for apoptosis to continue (Deveraux, 1997). It is important to note that XIAP's ability to bind caspases is not sufficient to block apoptosis; XIAP's RING domain, which serves as an ubiquitin

ligase, is required for XIAP's ability to inhibit caspases, and consequently, apoptosis in vivo (Joazeiro, 2000; Schile, 2008). Therefore, a critical step in carrying out apoptosis is the inhibition of XIAP.

As mentioned earlier, Smac/Diablo and Omi/HtrA2 are two pro-apoptotic proteins that are released from the mitochondria after MOMP. Once released, Smac/Diablo and Omi/HtrA2 are thought to bind to and inhibit XIAP, which in turn liberates caspases for the induction of apoptosis (Du, 2000; Martins, 2001; Verhagen, 2000). In addition, there is evidence that the interaction of Smac/Diablo and Omi/HtrA2 with XIAP promotes the ubiquitination and degradation of XIAP (Fu, 2003). This loss of XIAP inhibition of caspases along with caspase activation marks the final steps in the apoptosis cascade. However, it is important to note that there is no *in-vivo* evidence that supports Smac/Diablo's antagonistic role against XIAP or that it affects apoptosis *in-vivo*, since mice that are knocked out for Smac/Diablo do not have any apoptosis defects. These findings suggests that perhaps other pro-apoptotic factors are more important for the inhibition and degradation of XIAP.

A pro-apoptotic protein that is known to be involved early in apoptosis is the Septin 4 splice variant ARTS (Larisch, 2000). ARTS, which is usually localized at the mitochondria, is found in the cytosol as early as 30 minutes following staurosporine treatment. It has also been shown that ARTS can directly bind to and antagonize XIAP (Bornstein, 2011; Gottfried, 2004). In addition, unlike the other XIAP antagonists, ARTS interacts with XIAP well before MOMP (Edison, 2012). This suggests that ARTS is encouraging cell death very early in the apoptosis decision making process. Interestingly, ARTS has recently been implicated in stem cell apoptosis (García-Fernández et al., 2010). In a mouse skin wound healing model, it has been shown that the number of hair follicle stem cells increases when ARTS is knocked out, and consequently, the

mice are able to heal quicker after wounding due to the increased number of stem cells (Figure 1.2).

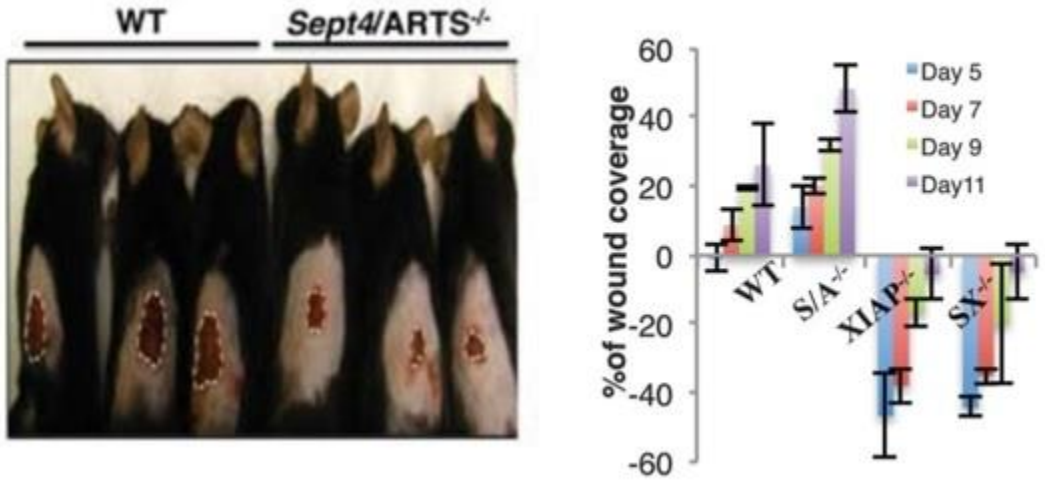

Figure 1.2: ARTS and XIAP play a pivotal role in stem cell homeostasis and wound healing. ARTS and XIAP play an important role in the regulation of apoptosis, with a particularly significant role in stem cell homeostasis. In this study, mice that were either wild-type, ARTS knockout, XIAP knockout or ARTS XIAP double knockout were given puncture wounds in the skin and their healing analyzed. Interestingly, mice that were ARTS knockout had more stem cells, and consequently, were able to heal their wounds quicker. In contrast, mice that were XIAP knockout had fewer stem cells and their wounds initially worsened before recovering. Finally, ARTS XIAP double knockout mice had the same phenotype as the XIAP knockout, showing that ARTS regulates stem cells via XIAP. These data are exciting because they highlight the critical role ARTS and XIAP play in stem cell biology. WT: Wild Type; S/A: ARTS; SX; ARTS/XIAP (Fuchs et al., 2013).

Knocking out XIAP in the ARTS deficient mice results in the opposite phenotype; the XIAP/ARTS double knockout mice have fewer stem cells and the wounds initially get larger, thus giving *in vivo* evidence that ARTS and XIAP have opposite functions in stem cell apoptosis (Fuchs, 2013). These recent *in vivo* stem cell findings are exciting because XIAP and ARTS have a more pronounced impact on apoptosis in these systems compared to their effect on cultured cell lines.

KINETICS OF APOPTOSIS

An intriguing observation of apoptosis is the fact that even within the same cell culture plate, cells can have significant variation in the time they take to undergo apoptosis, despite all conditions being the same between the cells (Figure 1.3).

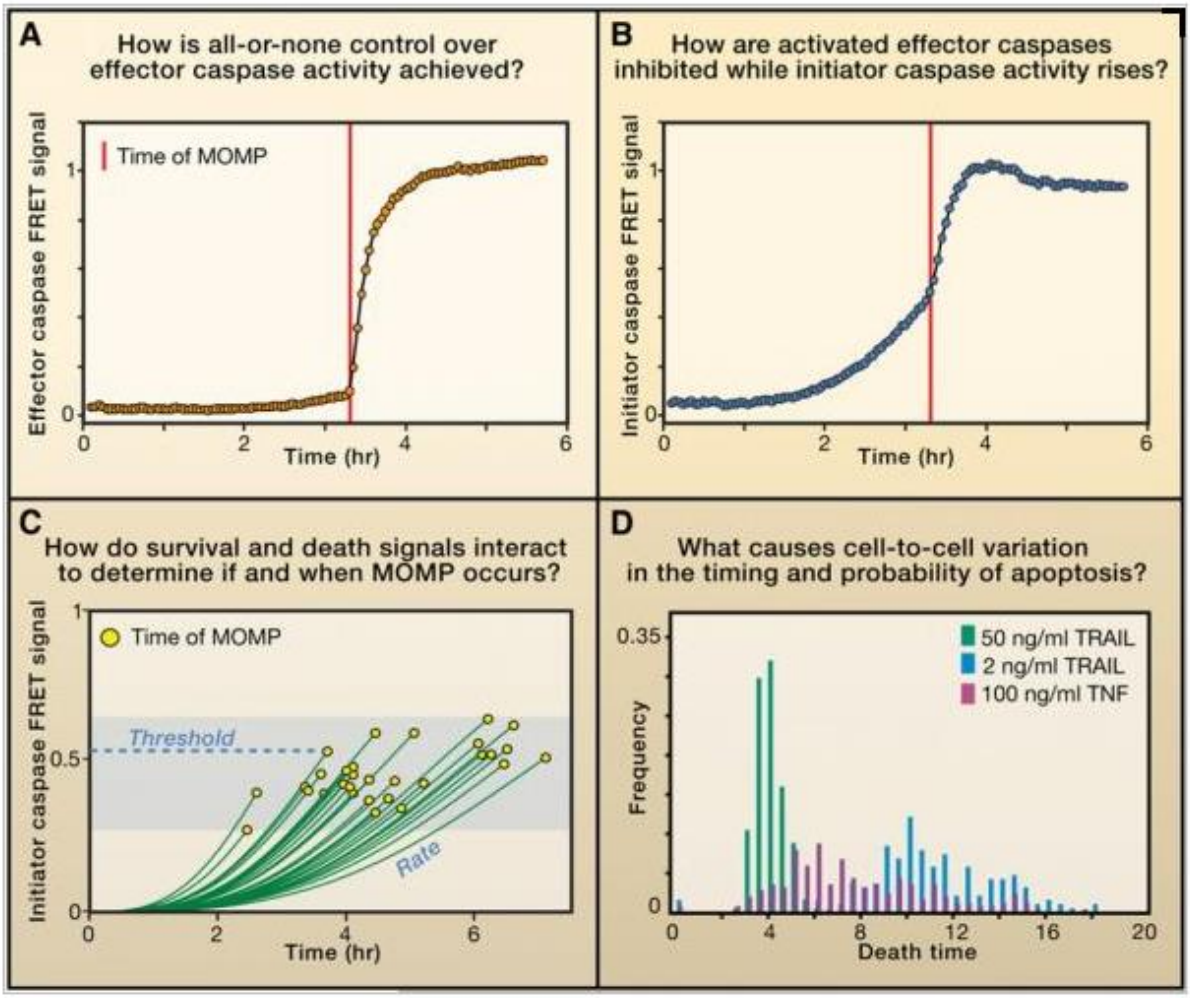

Figure 1.3: The kinetics of apoptosis at single-cell resolution.
When apoptosis is analyzed by western blot, it appears to be a predictable process with little variation; this is a result of western blots averaging an entire cell population. However, when using single-cell resolution, the temporal variation of apoptosis between cells becomes apparent. Mitochondrial outer membrane permeabilization (MOMP) is a committal step in apoptosis. After MOMP occurs, as is shown in panel A, the remaining apoptotic pathway becomes robust and predictable. However, large variation can exist in the time it takes individual cells to undergo MOMP, as shown in panel C. Although the majority of cells take around four hours to undergo MOMP, some cells can take as little as two hours or upwards of 20 hours, despite all of the cells receiving the exact same treatment. The goal of this project is to understand what accounts for the kinetic variation of apoptosis that is observed upstream of MOMP (Spencer & Sorger, 2011).

Usually, the average of the entire cell population is studied by looking at protein changes via Westerns blots. By looking at the population average, one would be mislead into believing that apoptosis is a very gradual process with little variability. However, after looking at the kinetics of apoptosis with single cell resolution, one can see that there is a large kinetic variance that occurs between cells undergoing apoptosis. When given staurosporine or TRAIL, most cells will undergo MOMP in 3-4 hours; however, some cells in the plate will take up to 16 hours or even longer to undergo MOMP. In addition, the time it takes for MOMP and cytochrome C release can vary greatly based on the death-inducing stimulus. For example, it takes approximately 3-4 hours for MOMP to occur when a cell is given staurosporine or TRAIL, compared to 14 hours for UV-induced death (Goldstein, 2005). Furthermore, it has been shown that stronger doses of UV induce apoptosis in cells quicker than weaker doses (Goldstein, 2000). Figure 1.3D shows the temporal variance that occurs between individual cells undergoing apoptosis, despite the fact that they are in the same dish. By studying early, decision-making events, we hope to give insight into the mechanism that accounts for the kinetic variability between dying cells.

CHAPTER 2: MATERIALS AND METHODS

Cell culture of human cancer cell lines

HeLa and MCF7 cells were acquired from ATCC. ARTS knockdown HeLa cells were derived from the Larisch lab of Haifa University. The human cell lines were grown in DMEM containing 10% FBS at 37 Celsius with 5% CO2.

Cell culture of mouse keratinocytes and HFSCs

Keratinocytes and HFSCs were obtained from WT, ARTS KO and XIAP KO mice. The protocol for harvesting the keratinocytes and HFSCs is as described by (Soteriou et al., 2016). The HFSCs and keratinocytes were grown in low calcium conditioned media provided by Elaine Fuchs's lab and grown at 37 Celsius at 5% CO2.

Generation of stable shRNA knockdowns in mouse keratinocytes

Neurl4, XIAP, Herc2 and SSSCA1 were knocked down in keratinocytes using a lentiviral shRNA library provided by the Elaine Fuchs lab. The protocol for the lentiviral knockdown is described by (Beronja, Livshits, Williams, & Fuchs, 2010).

siRNA knockdowns in human cancer cell lines

The RNAiMAX kit from Thermo Fischer was used for the transfections of the siRNAs. In brief, the cells were incubated with 10nM of each siRNA for 24 hours and then used for assays.

The siRNAs used are as follows: ARTS 5' - GAGCACCAGGGGCAGGGCT - 3'; Apaf1 5' – AATTGGTGCACTTTTACGTGA – 3'; Herc2 ON-TARGETplus Human HERC2 (8924) siRNA – Individual from Dharmacon; Neurl4 ON-TARGETplus Human NEURL4 (84461)

siRNA – Individual from Dharmacon; XIAP custom VC30002 XIAP siRNA from QIAGEN XIAP siRNA #5 sequence; SSSCA1 SASI_Hs01_00114866 SSSCA1 siRNA Rank 1 from Sigma Aldrich.

Induction of apoptosis by STS, ETO and UV

Apoptosis was induced in cells using varying concentrations of STS, ranging from 0.05-5uM. The STS was added directly to the cells by pipetting into the media. ETO was used at a concentration of 50uM and incubated for varying amount of time, ranging from 12-72 hours. Cells were induced to die with UV using the STRATALINKER 2000 crosslinker with 200uJ of UV. Cells would typically die after 12-24 hours after exposure.

Collecting apoptotic cells for IP and gel filtration

When cells were ready to be collected, the media would be collected and spun down to catch any detached cells. Then, the cells would be washed with PBS and trypsinized with 0.25% trypsin for 5-10 minutes. The cells would then be added to the same tube containing their corresponding media and spun for 5 minutes at 800g. The cell pellet would then be washed with freeze-thaw lysing buffer (50mM PIPES, 50mM NaCl, 2mM EGTA, 1mM magnesium chloride) and spun again. Finally, the cells would be resuspended at a 1:1 ratio of freeze-thaw lysis buffer to pellet volume. The cells would then be lysed by freeze thaw: the cells would be flash frozen in liquid nitrogen for 30 seconds, then thawed in 9 Celsius water for a total of 3 freeze/thaws. The lysis would then be spun at 20,000g for 10 minutes at 4 Celsius. The supernatant would then be transferred to a new tube and spun again. The supernatant is now ready for IP or gel filtration.

Gel filtration

Cell lysates were fractionated using the following columns: Superdex 200 10/30GL, Sephacryl S500 100/300GL. The Akta Pure 25 HPLC system was used for gel filtration. All gel filtrations were done at 4 Celsius. The buffer used for gel filtration is: 50mM PIPES, 150mM NaCl, 2mM EDTA, 1mM magnesium chloride.

IP and mass spectrometry

Following gel filtration, the fractions containing the complex were identified by Western Blot. The fractions containing the complex were then pooled together into the same tube and IPed using magnetic DynaBeads covalently conjugated to antibodies. The antibodies used were: SSSCA1 ab117911 Anti-SSSCA1 antibody [2F5] from Abcam; Neurl4 PRX-MKA1787 from Cosmo Bio; Herc2 612366 from BD Transductions; ARTS monoclonal mouse from Sigma; XIAP clone 28 from BD Transductions.

100ng of beads were used per 1ml of IP. The fractions were incubated with the beads for 4 hours at 4 Celsius while rotating. The beads were then washed 8 times with cold PBS and eluted with 50ul of 8M urea. The 50ul eluate was then used for in-solution mass spectrometry and compared to the IP of fractions containing the 440kDa XIAP complex.

Time lapse imaging of apoptosis

For time lapse live imaging of cells, the incubator Fluffles microscope at the Rockefeller University Imaging Facility was used. To visualize apoptosis in real time, the cells were given the fluorescent caspase 3/7 indicator CellEvent™ Caspase-3/7 Green Detection Reagent from Invitrogen. The protocol provided by the kit was followed. In addition, the cell nuclei were

stained using SiR-DNA (Cat. # CY-SC007) from Cytoskeleton. After the cells were induced to die, they were imaged for various amounts of time using a DIC objective for the cell body, a GFP objective for the caspase indicator and a Cy5 objective for the SiR-DNA signal. The number of apoptotic cells was determined by dividing the total number of green cells (caspase positive cells) by the total number of Cy5 positive cells (SiR-DNA Cy5 stains all cells regardless of apoptosis).

Drosophila melanogaster wing disc experiments

The wing discs from wandering third instar larva were dissected and treated with staurosporine in Schneider's media. The wing discs were then fixed with 4% paraformaldehyde for 1 hour at room temperature. The fixed wing discs were then stained with Hoechst, anti-cleaved Caspase 3 antibody (Cell Signaling 9661) and anti- γ-H2Av antibody (DSHB UNC93-5.2.1) and imaged by immunofluorescence.

CHAPTER 3: XIAP IS RECRUITED TO A LARGE COMPLEX DURING APOPTOSIS

Identifying proteins involved in the initiation of apoptosis

Early events in the initiation of apoptosis are poorly understood. As mentioned earlier, the kinetics of apoptosis varies widely between individual cells. However, after MOMP, the execution and time frame of apoptosis becomes very robust and predictable, with little variation; all of the kinetic variance occurs upstream of MOMP. Therefore, in order to study apoptosis during these upstream, decision-making events, we decided to look for changes using gel filtration in canonical apoptosis proteins immediately after inducing cells to die with staurosporine (STS).

Because it has been shown that ARTS is upregulated within 30 minutes of STS-treated cells, we looked for ARTS-dependent changes of other apoptosis proteins at similar time points. We discovered that a small portion (approximately 1%) of the total XIAP is recruited to a large complex within 30 minutes of STS-treated HeLa cells (Figure 3.1).

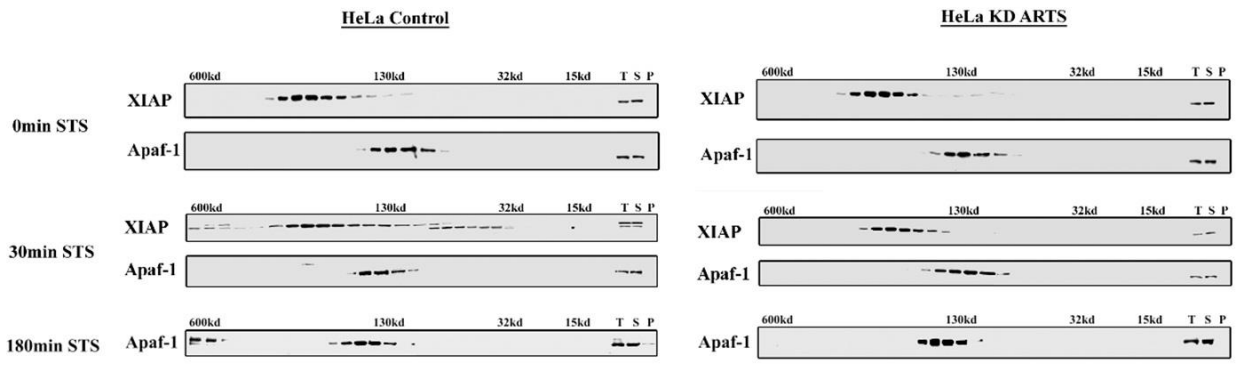

Figure 3.1: A large XIAP-containing complex forms in the first 30 minutes of apoptosis. HeLa cells were treated with 1.75uM STS for 30 minutes and then lysed by freeze thaw. The soluble lysate fraction was run on a Superdex 200 gel filtration column. These data show that XIAP is recruited to a large complex 30 minutes after STS treatment and this recruitment is dependent on ARTS, since XIAP is not recruited to the complex in the ARTS knockdown cells. The apoptosome formation is also delayed in the ARTS knockdown cells, showing that ARTS, and perhaps XIAP's recruitment to the large complex, is important for proper apoptosis initiation.

Importantly, the knockdown of ARTS abrogates the recruitment of XIAP to the complex, suggesting that the recruitment of XIAP to this large complex is dependent on ARTS and specific to apoptosis. Furthermore, the knockdown of ARTS also delays the formation of the apoptosome (a complex containing Apaf-1), perhaps because the recruitment of XIAP to this complex might be a required step for downstream apoptotic events to occur properly.

Elucidating the molecular size of the complex

Although we observe XIAP being recruited to a large complex, the fractions that contain the complex are in the flowthrough of the initial column used. In other words, the size of the complex is beyond the upper resolution limit of the column. Therefore, in order to elucidate the actual size of the complex that XIAP is being recruited to, we shifted to a larger column. Repeating the same method using the larger column, we discovered that the complex XIAP is

being recruited to is approximately 5MDa in size. Specifically, we see that the complex XIAP is recruited to peaks at fraction 16, which is much larger than the proteasome (Rpt3), which is around 2MDa and peaks at fraction 22 (Figure 3.2).

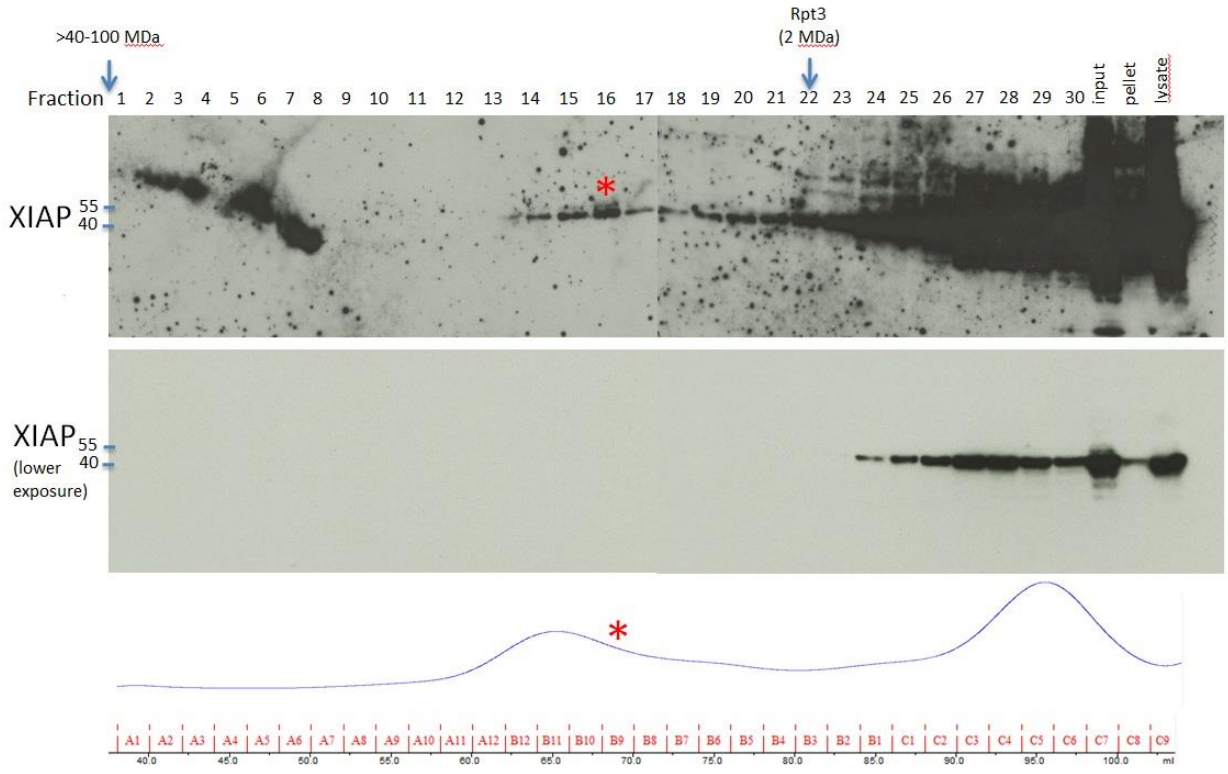

Figure 3.2: The large XIAP-containing complex is approximately 5MDa.
HeLa cells were treated with 1.75uM STS for 30 minutes and then lysed. The soluble lysate fraction was run on a Sephacryl S500 gel filtration column. (Top two panels) The fractions were then blotted for XIAP by western. (Lower panel) Chromatogram of lysate using absorbance at 280nm. Because the first column (Superdex 200) used has a size resolution limit of 600kDa, we switched to a larger column and discovered that the complex XIAP is recruited to during apoptosis is approximately 5MDa. The red asterisk indicates the peak fraction containing the 5MDa complex. The peak fraction that would contain the 26S proteasome (Rpt3) is marked to show where a 2MDa complex would elute on this column.

After discovering that the molecular size of the complex is approximately 5MDa, we next wanted to test the complex's stability in detergent. Because such a minute amount of total XIAP

is recruited to the complex, it would be useful to know whether detergent can increase the amount of the complex that can be recovered from the cell lysate. We added the mass spectrometry-compatible detergent PPS Silent Surfactant in varying quantities to the cell lysates before running the lysates on the column (Figure 3.3).

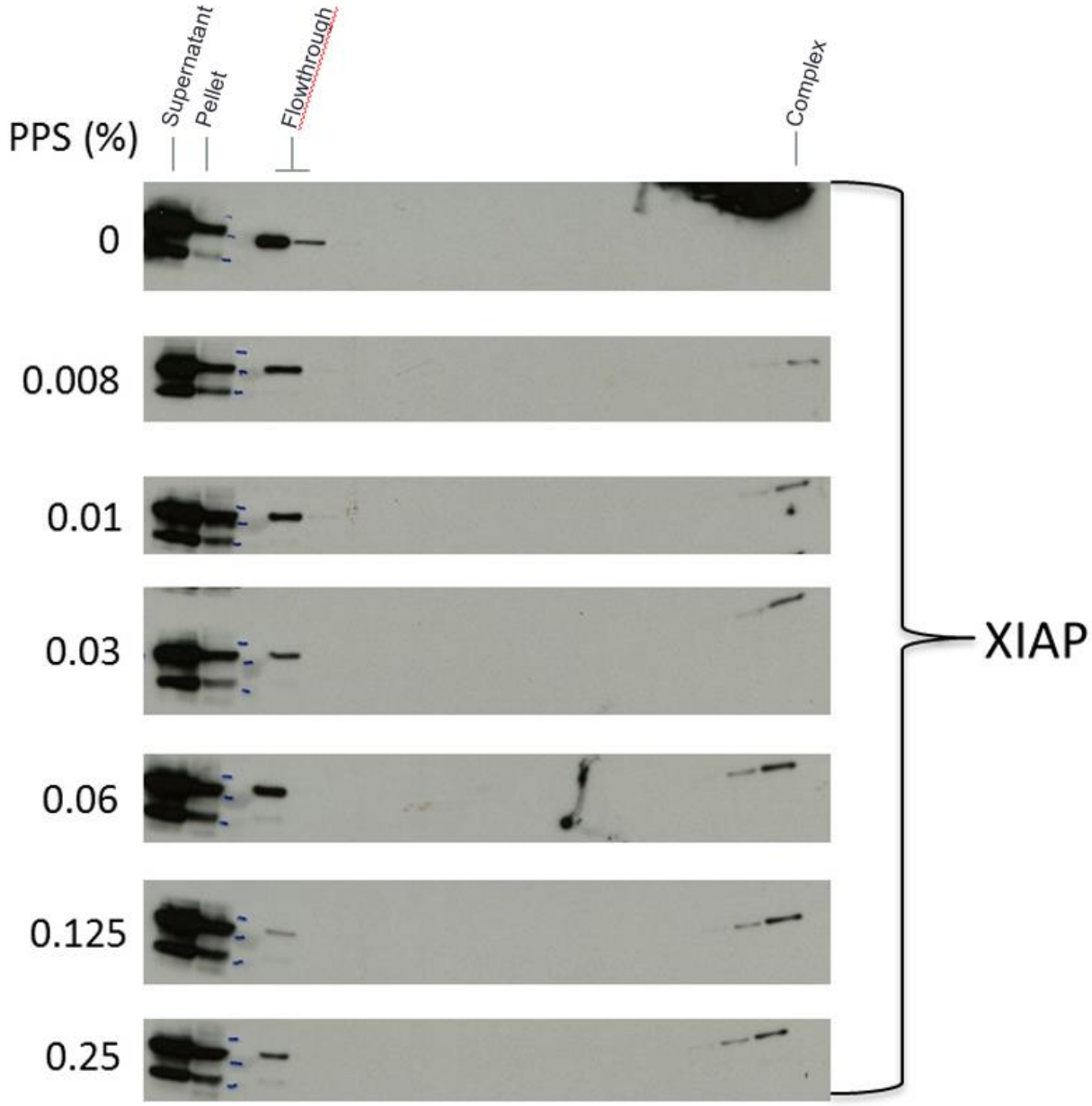

Figure 3.3: PPS Silent Surfactant does not increase the yield of the complex during purification. HeLa cells were lysed by freeze thaw and treated with varying amounts of PPS Silent Surfactant. The supernatants of the lysates were then run on the sephacryl S500 gel filtration column. PPS Silent Surfactant did not affect the amount of the complex that could be obtained, nor did it disrupt the stability of the complex. These data suggest that the complex's stability is resistant to detergent and detergent does not increase its solubility, since the amount of XIAP in the pellet did not change.

Adding the detergent PPS Silent Surfactant did not increase the solubility of the complex and did not disrupt the stability of the complex as well. As can be seen in Figure 3.3, the vast majority of XIAP is in the supernatant, with very little in the pellet. However, it is unknown how much of the XIAP in the pellet is composed of the 5MDa apoptosis complex versus the 400kDa complex, which contains the vast majority of XIAP and is not apoptosis dependent. Since the pelleted-XIAP was not affected by the PPS detergent, other methods, such as varying the salt concentration of the lysate, can be used to determine if the amount of pelleted-XIAP can be altered.

Now that we have discovered the true size of the complex using the Sephacryl S500 column, we wanted to test if other canonical apoptosis proteins are eluting in the same fractions. The obvious candidate to test first is ARTS, since the formation of the complex is ARTS-dependent. However, to our surprise ARTS was detected in the 5MDa fractions (Figure 3.4).

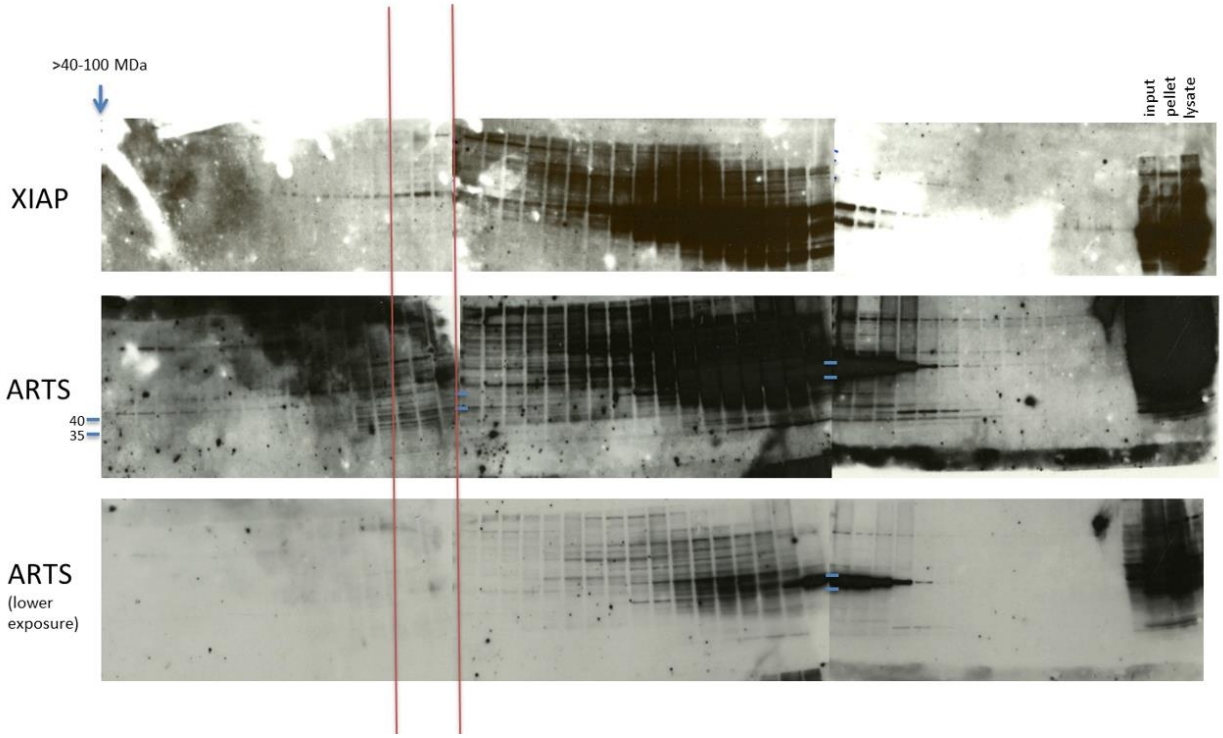

Figure 3.4: ARTS is not detected in the 5MDa fractions.
STS-treated HeLa cells were lysed and fractionated by gel filtration using the S500 column. We looked for the presence of ARTS in the 5MDa fractions (inside the vertical red lines) since the formation of the complex is ARTS-dependent. ARTS was not detected in the 5MDa complex, suggesting that ARTS is not physically bound to the complex, despite being involved in its formation.

Although the formation of the 5MDa complex is dependent on ARTS, ARTS itself was not detected in the fractions containing the complex. This result suggests that ARTS is not physically associated with the complex. Alternatively, the association of ARTS with the complex could be extremely transient, resulting in levels of ARTS that are not detectable by Western Blot or that the association does not persist through the gel filtration procedure. Since ARTS was not observed to be physically bound to the complex, perhaps it acts as a chaperone to bring the various subunits of the complex together. Another explanation is that ARTS is necessary for post-translational modifications of the subunits in order to allow the formation of the complex.

Mass spectrometry is significantly more sensitive than Western Blots, so if ARTS is bound to the complex in quantities not detectable by Western Blot, it should be detectable by mass spectrometry. Mass spectrometry could also potentially tell us if the subunits of the complex are post-translationally modified compared to the unassociated subunits. However, mass spectrometry becomes more complex when looking for protein modifications and requires large quantities of the modified proteins, which is a problem given that the amount of the total XIAP in the complex is miniscule in comparison to the total XIAP. Therefore, we wanted to first look by Western Blot to determine if there are noticeable size shifts in XIAP compared to the unassociated XIAP to determine if XIAP is perhaps modified in the complex (Figure 3.5).

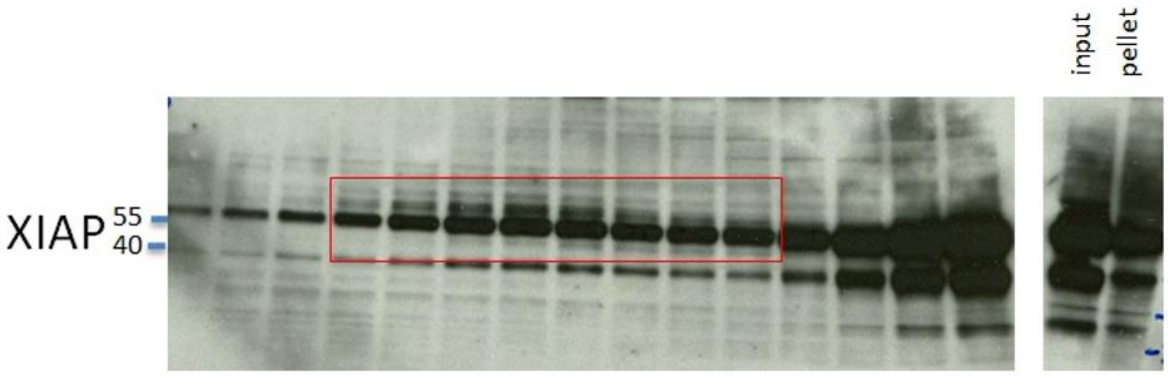

Figure 3.5: XIAP appears to be post-translationally modified in the complex. STS-treated HeLa cells were lysed and fractionated by gel filtration using the S500 column. XIAP in the 5MDa fractions (outlined in the red rectangle) was then visualized by Western Blot. A ladder of increasing size of XIAP can be seen in the 5MDa fractions, showing that XIAP is post-translationally modified in the complex. The size of the XIAP ladder bands are approximately a few Daltons each, suggesting a large modification such as ubiquitination.

Looking closely at XIAP in the 5MDa fractions, it does appear that XIAP is being post-translationally modified. A ladder of increasing size of XIAP can be seen in the fractions containing the complex. The size increase of the modified XIAP is a few Daltons each,

suggesting a large modification, such as ubiquitination. Since ubiquitination is suspected, the next step would be to purify the complex by immunoprecipitation and blotting for ubiquitin to determine if the modification is indeed ubiquitin or some other modification. Importantly, the ladder must be due to a modification and is not due to breakdown of XIAP, since all of the steps of the ladder are above the endogenous size of XIAP (~55kDa).

In addition to ARTS, we wanted to test whether other canonical apoptosis proteins could be found in the fractions containing the complex (Figure 3.6). Looking through the literature, we compiled a table of all proteins known to be able to bind to XIAP (Table 3.1).

Table 3.1: A list of all known XIAP interactors.
We went through the literature of XIAP to compile a table of all validated interactors of XIAP. Most of the proteins were identified by large-scale proteomics studies. This table can be used to find potential candidates that compose the 5MDa complex.

Proteins known to bind XIAP

Multiple Source Validation

NAME	kDa
NOD2	155
USP19	146
Apaf1	140
Rip4	86
TBK1	84
TLE3	83
TCF25	77
UBC	77
Rip1	76
LATS1	76
Raf1	73
BIRC2/cIAP1	68
AIFM1	67
MAP3K7	67
Rip2	61
TRAF6	60
Rip3	57
Tab1	55
TCF7L2	51
PTEN	47
Omi/HtrA2	39
ELAVI	36
Caspase 9	35
XAF1	35
PGAM5	32
ARTS	31
CCS	29
SMAC/Diablo	27
SERTAD1	25
COMMD1	21
Caspase 7	20
Caspase 3	20
UBE2D3	17
UBE2D1	17
UBE2W	17
Survivin/BIRC5	16

Single Source Validation

NAME	kDa	NAME	kDa
NOTCH1	273	AHCY	48
BRCA1	208	STRADB	47
USP19	146	SSB	47
PFAS	145	E2F1	47
INPP5D	133	GSK3B	47
ERC1	128	IRF3	47
LATS1	127	CASP4	43
SEC23IP	111	HNRNPA1	39
USP11	110	DTX3	38
USO1	108	STUB1	35
NOD1	108	HNRNPC	34
EXTL3	105	BIRC7	33
USP5	96	HAX1	32
RIPK4	92	SIAH1	31
MAGED1	86	TOLLIP	30
IKBKE	80	UCHL3	26
TCF25	77	BCL10	26
TAB2	76	SERTAD1	25
TRIM32	72	ARHGDIA	23
MAP3K2	70	BAX	21
HSPA4	70	RAC1	21
BIRC3	68	SIVA1	19
ATP6V1A	68	NUDCD2	17
AFP	67	UBE2N	17
SCARA3	65	UBE2V2	16
TRIM8	61	UBE2V1	16
CCT2	57	NEDD8	9
RIPK3	57		
BMPR1B	57		
AKT1	56		
AKT2	56		
TRAF2	56		
MDM2	55		
GSPT1	55		
CHEK1	54		
HTRA1	51		

Using Table 3.1, we looked by Western Blot for validated XIAP interactors in the 5MDa fractions for which we had antibodies (Figure 3.6).

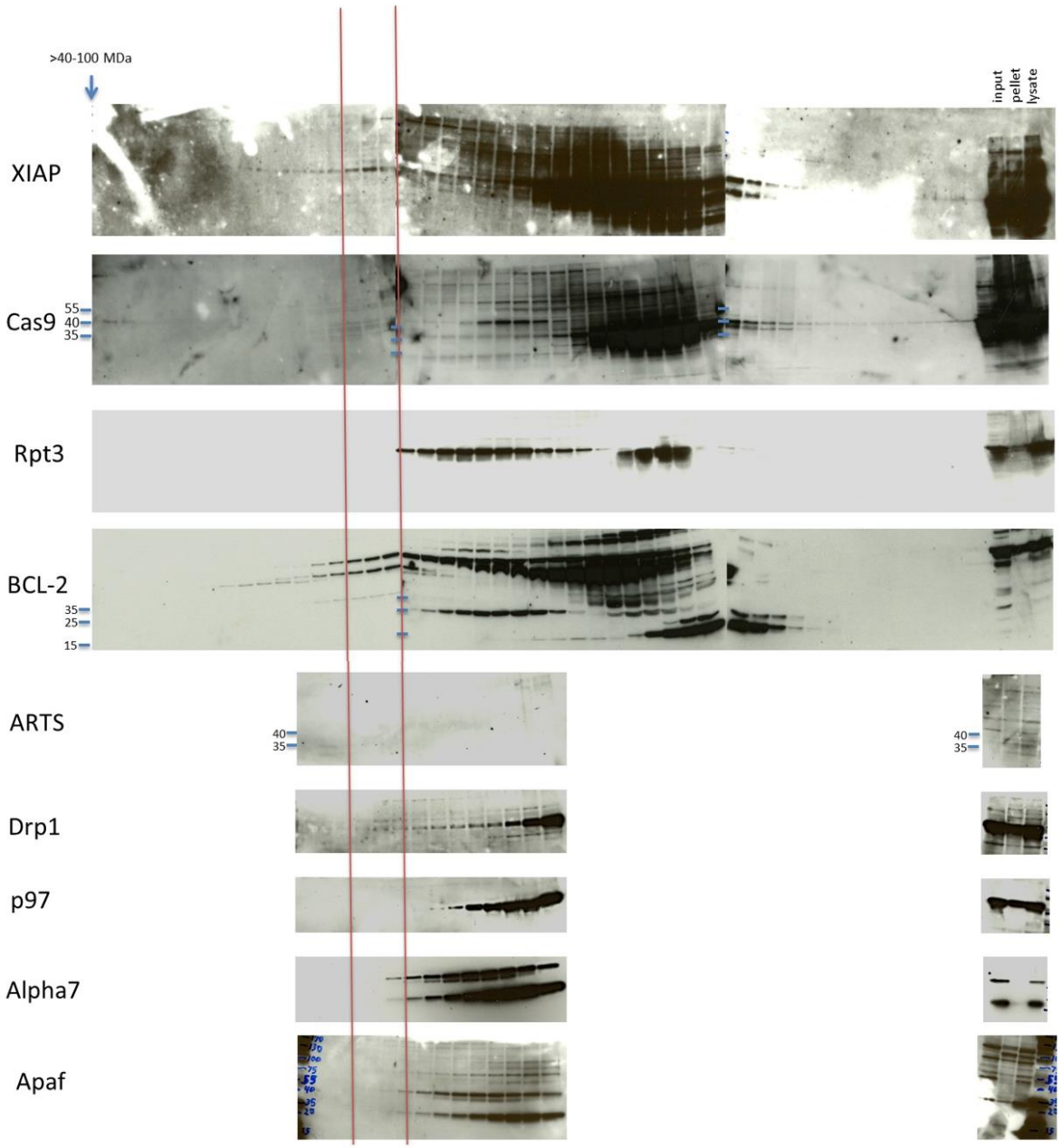

Figure 3.6: Co-elution of other canonical apoptosis proteins with the 5MDa complex. STS-treated HeLa cells were lysed and fractionated by gel filtration using the S500 column. We looked for the presence of various proteins in the 5MDa fractions (inside the vertical red lines) to search for potential subunits of the complex. None of the proteins analyzed co-eluted with the 5MDa complex.

None of the proteins we looked at co-eluted with the 5MDa complex. Some of the proteins are canonical apoptosis proteins, such as Caspase 9, BCL-2, ARTS and Apaf. Others, such as p97

and Drp1 are chaperones that could potentially be involved in the formation of the complex. Rpt3 is part of the proteasome and is a useful size marker, peaking in fractions approximately 2.6MDa in size. In addition, due to the large size of the complex, we were interested to determine if the proteasome could be part of it and contribute to its large size. However, as was the case with all of the proteins tested so far, Rpt3 also did not co-elute with the 5MDa complex.

Co-immunoprecipitation and identification of the complex by mass spectrometry.

So far, the only known component of the complex is XIAP. To identify the other subunits, we co-IPed the complex from the Sephacryl S500 gel filtration fractions containing the complex with anti-XIAP antibody conjugated beads. As a control, we used beads conjugated to random mouse IgG antibodies. The strategy we used for the mass spectrometry is shown in Figure 3.7.

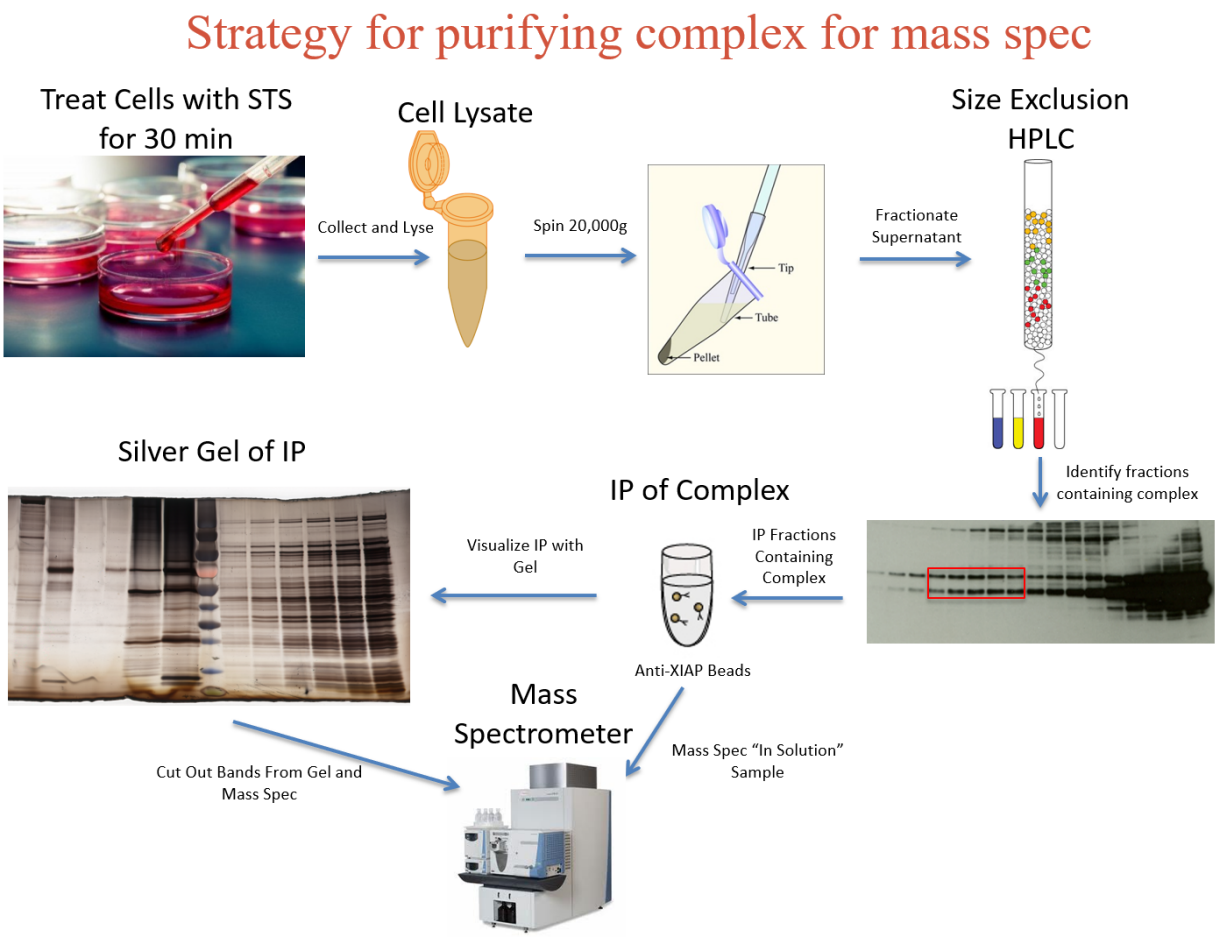

Figure 3.7: The strategy used for the mass spectrometry experiment. STS-treated HeLa cells will be lysed and fractionated by gel filtration using the S500 column. The fractions containing the complex (outlined in red) will then be immunoprecipitated for XIAP and sent for mass spectrometry by both silver gel and solution. The results of both the silver gel and in-solution mass spectrometry should identify the subunits of the complex. The control for the mass spectrometry will be immunoprecipitation of the same fractions using purified mouse IgG antibodies.

Before doing the mass spectrometry, we first have to validate the immunoprecipitation of XIAP and its elution by mass spectrometry-compatible methods. The two most common ways to elute protein from antibody for mass spectrometry are by using glycine and urea. We tested both methods to determine which one works better (Figure 3.8).

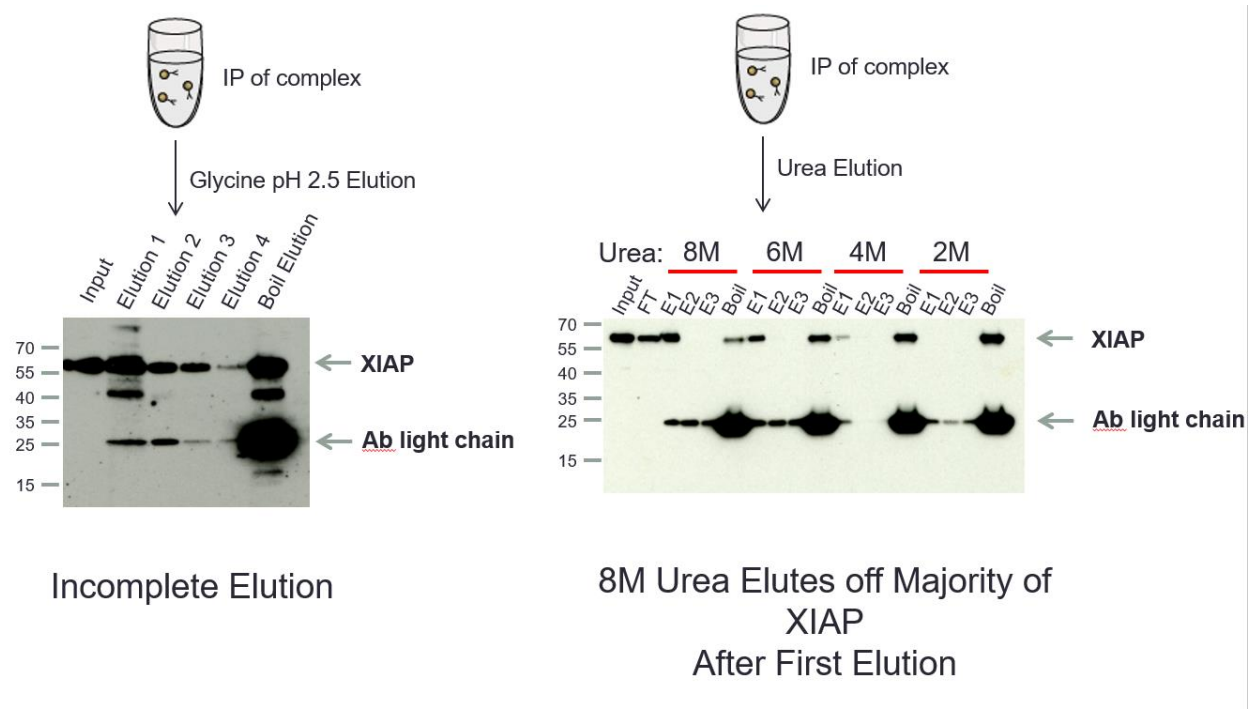

Figure 3.8: Validating the elution of the anti-XIAP IP by glycine and urea for mass spectrometry.
STS-treated HeLa cells will be lysed and fractionated by gel filtration using the S500 column. The fractions containing the complex were then immunoprecipitated for XIAP (clone 48 antibody) and eluted by the addition of either glycine pH 2.5 or urea. The glycine pH 2.5 resulted in incomplete elution of XIAP from the antibody whereas the 8M and 6M urea fully eluted XIAP in a single elution. Therefore, urea is a much better method of elution when eluting XIAP from the clone 48 antibody compared to glycine. FT = flowthrough; E = elution.

The glycine pH 2.5 did not fully elute XIAP from the antibody. In contrast, 8M and 6M urea fully eluted XIAP in a single elution. The upper limit of urea that is still suitable for mass spectrometry is 8M, which is the concentration we have decided to use for the mass spectrometry experiment. If neither the glycine or urea worked well, we would have to either use a different antibody for the IP or use a harsher method of elution, which usually results in higher noise.

However, one method of elution that works well without producing more background noise is using a peptide competitor that competes with the protein binding interface of the antibody. In order to develop a peptide that can compete for the antibody, one must first identify the epitope on the protein that is recognized by the antibody. In addition for mass spectrometry, elution by a

peptide competitor is useful for *in vitro* assays, as it does not disrupt or denature the proteins, thus preserving their function. Therefore, we aimed to identify the epitope of XIAP that is recognized by the antibody so that we could produce a peptide that can be used for elution (Figure 3.9).

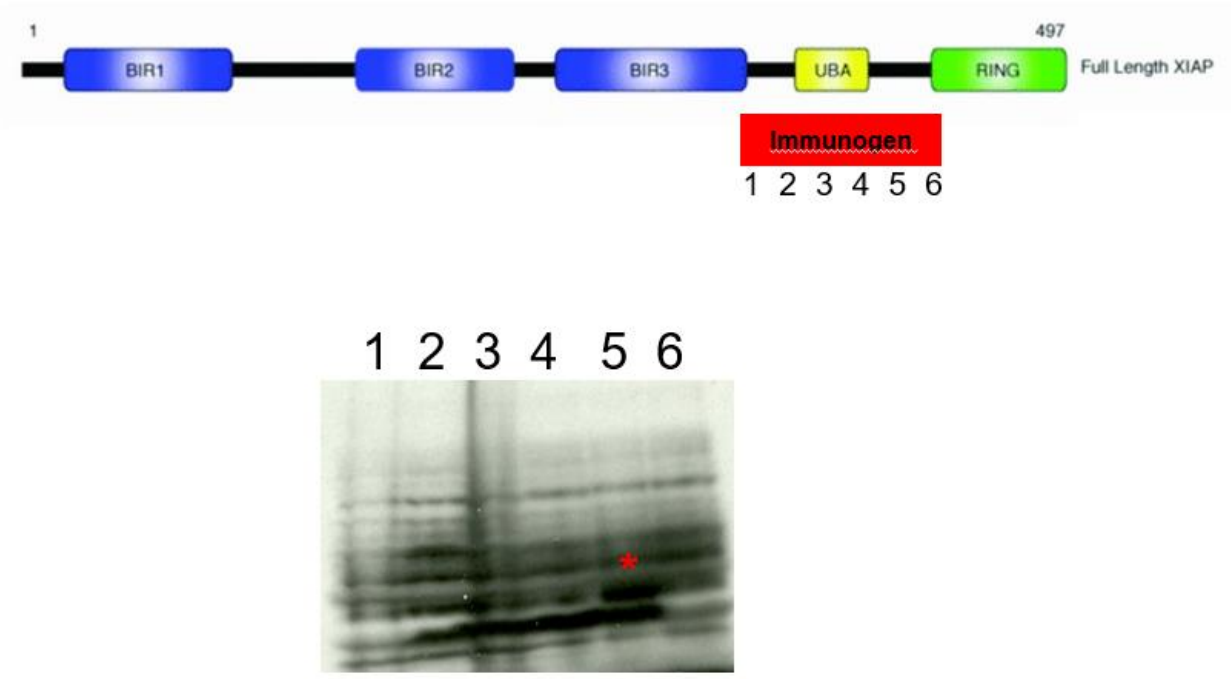

Figure 3.8: Determining the XIAP epitope that is recognized by the antibody.
The peptide used to produce the antibody (anti-XIAP clone 48 by BD Transductions) maps to the UBA domain of XIAP. In order to find the exact epitope, we divided the immunogen peptide into six different fragments. We then cloned and purified each fragment and tested which of the six fragments could be immunoprecipitated by the antibody. We discovered that fragment five was able to bind to the antibody. The identified epitope can be used as a peptide competitor to elute XIAP from the antibody without denaturing proteins.

The company that produces the antibody provided the peptide that was used to generate the antibody, which mapped to the UBA domain of XIAP. In order to make a precise peptide competitor, we divided the peptide into six fragments and tested which of the fragments could bind to the antibody. We discovered that the fifth fragment was able to be pulled down by the

antibody. The identification of this peptide provides us a way to elute XIAP and the complex from the antibody for *in vitro* functional assays that require the proteins to be in their native form.

Mass spectrometry identification of the complex

Moving forward with the mass spectrometry experiment, we used the strategy mentioned above (Figure 3.9).

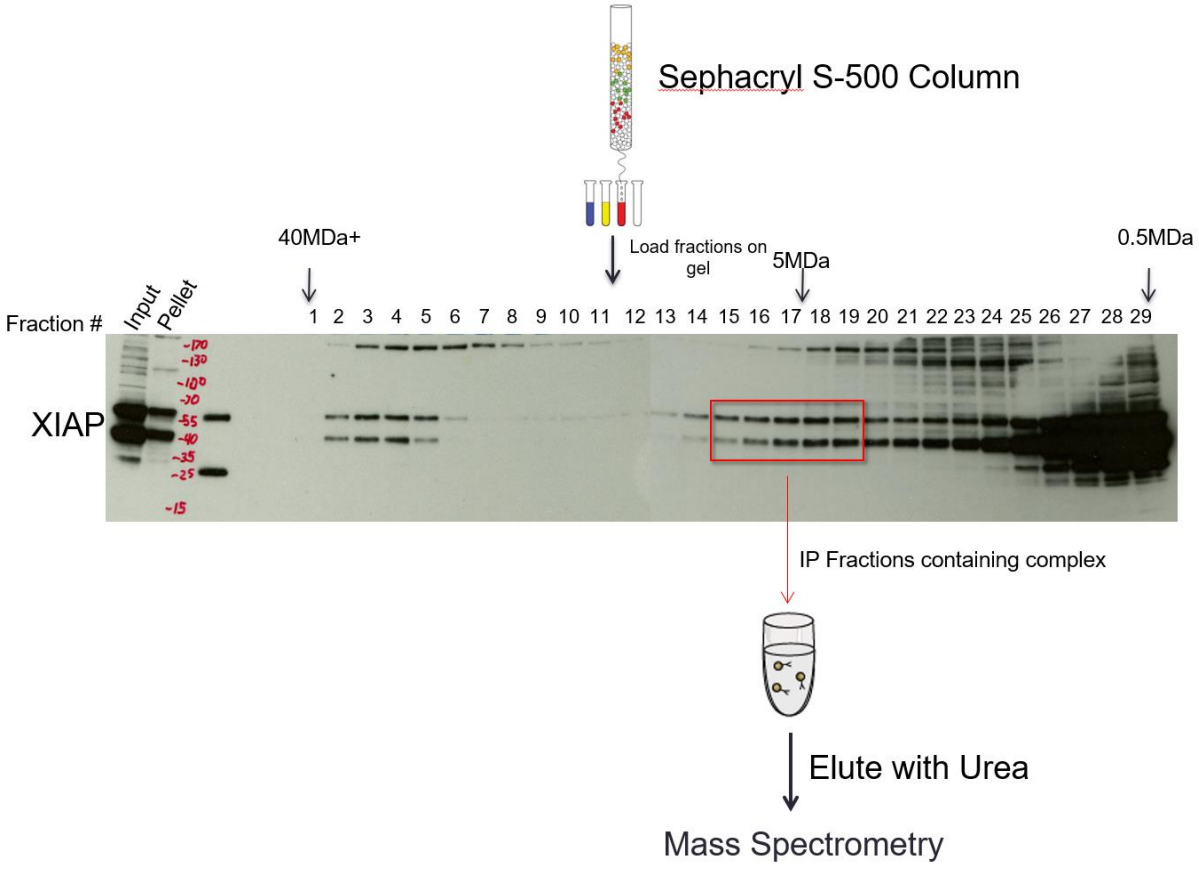

Figure 3.9: The mass spectrometry experiment.
STS-treated HeLa cells were lysed and fractionated by gel filtration using the S500 column. The 5MDa fractions were pooled together and the complex was pulled down by anti-XIAP Ab beads. The control consisted of the fractions being pulled down with mouse IgG antibody. The complex was then eluted from the antibody with 8M urea and used for mass spectrometry. The red rectangle indicates the fractions containing the 5MDa complex.

Interestingly, three of the proteins (Herc2, Neurl4 and SSSCA1) have been shown to form a complex with each other. However, Herc2, Neurl4 and SSSCA1 have not been previously shown to interact with XIAP, suggesting this is a newly discovered apoptosis-dependent interaction (Figure 3.8 and Figure 3.9).

Band Size	Mass Spec Identification	kDa
300	Myosin-9	226.4
300	E3 ubiquitin-protein ligase HERC2	526.9
250	Isoform 2 of Probable E3 ubiquitin-protein ligase MYCBP2	509.4
250	Isoform Numa-s of Nuclear mitotic apparatus protein 1	200.0
200	Neuralized-like protein 4 (Fragment)	153.2
120	E3 ubiquitin-protein ligase HERC2	526.9
100	Myosin-9	226.4
50	E3 ubiquitin-protein ligase XIAP	56.6
45	Myosin-9	226.4
40	Calmodulin-like protein 5	15.9
20	Sjoegren syndrome/scleroderma autoantigen 1 (Fragment)	21
10	Small nuclear ribonucleoprotein F	10

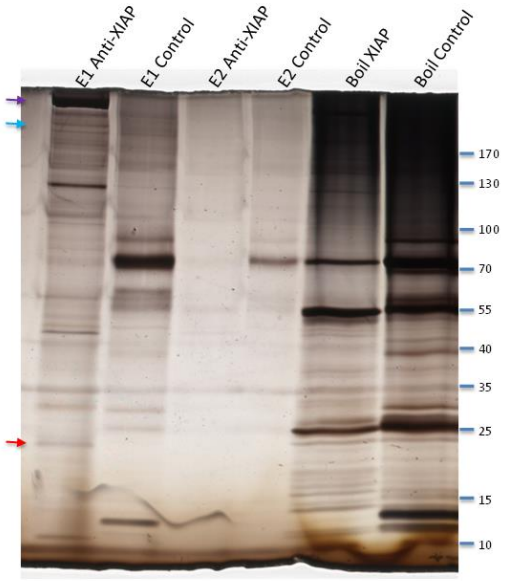

Figure 3.8: Silver gel mass spectrometry results of the 5MDa complex.
STS-treated HeLa cells were lysed and fractionated by gel filtration. The 5MDa complex was pulled down by anti-XIAP Ab beads, visualized and cut from a silver gel and identified by mass spectrometry. The color-coded arrows show the gel bands that correspond to the identified proteins. Herc2, SSSCA1 and Neurl4 were the most interesting proteins identified because they are not commonly found in mass spectrometry results and have been shown to interact with each other. E = Elution by 8M Urea. Boil = elution by boiling the beads.

Protein	Full name	kDa	Fold-enrichment over control	MS/MS Area
HERC2	E3 ubiquitin-protein ligase HERC2	527	72	4.653E7
SSSCA1	Sjoegren syndrome/scleroderma autoantigen 1	22	Unique	2.256E7
Smac/Diablo	Isoform 2 of Diablo homolog, mitochondrial	21	Unique	1.574E7
MYCBP2	Probable E3 ubiquitin-protein ligase MYCBP2	510	2.7	1.394E7
XIAP	E3 ubiquitin-protein ligase XIAP	57	Unique	1.248E7
NEURL4	Neuralized-like protein 4	164	Unique	1.103E7
SMC2	Isoform 2 of Structural maintenance of chromosomes protein 2	125	18.5	1.077E7
DnaJ	DnaJ homolog subfamily B member 1	38	Unique	1.071E7
SSBP	Single-stranded DNA-binding protein, mitochondrial	17	Unique	1.056E7

Figure 3.9: In-solution mass spectrometry results of the 5MDa complex.
STS-treated HeLa cells were lysed and fractionated by gel filtration. The 5MDa complex was pulled down by anti-XIAP Ab beads and identified by mass spectrometry. The red arrows point to proteins of interest, which have also been shown to interact with each other, but not with XIAP. These data are consistent with the silver gel mass spectrometry results in that Herc2, SSSCA1 and Neurl4 were also identified. SMAC is a mitochondrial protein that has been shown to bind XIAP, so it showing up in the results is not surprising. The remaining proteins are extremely abundant proteins that are commonly found in mass spectrometry results.

Although Herc2, Neurl4 and SSSCA1 are largely uncharacterized, they were the most interesting candidates to us because they were the most enriched compared to the control. The enrichment of the proteins identified by the mass spectrometry falls of significantly after SSBP (data not shown).

Co-elution of identified proteins with XIAP

Next, we wanted to see how the gel filtration elution profiles of the identified proteins matched with the elution profile of XIAP. Unsurprisingly, Herc2, Neurl4 and SSSCA1 can all be found in the same 5MDa fraction as XIAP (Figure 3.4).

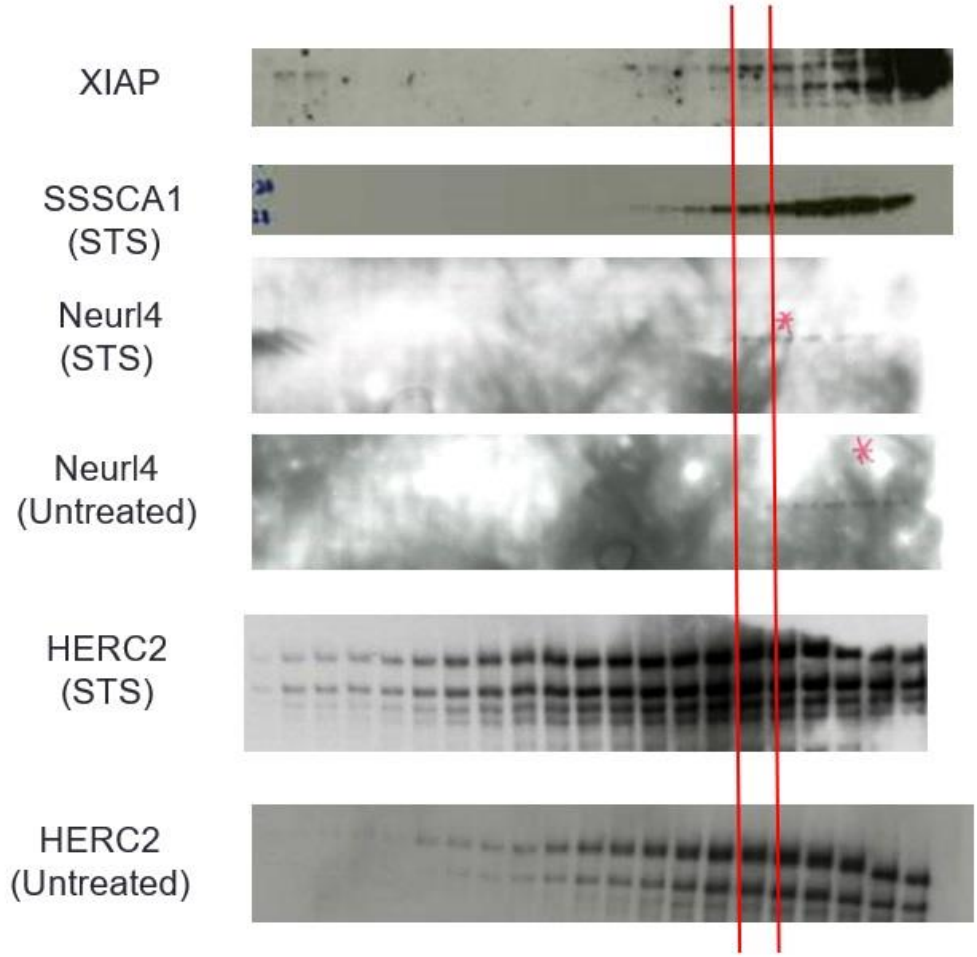

Figure 3.4: Co-elution of the identified proteins with the 5MDa complex.
STS-treated HeLa cells were lysed and fractionated by gel filtration using the Sephacryl S500 column. Westerns of Herc2, XIAP, Neurl4 and SSSCA1 were done on the fractions to compare their elution profiles. Not surprisingly, Herc2, SSSCA1 and Neurl4 were all found in the 5MDa fractions. The elution profile of Herc2 and SSSCA1 did not change with STS treatment (data not shown for SSSCA1). Interestingly, upon STS treatment Neurl4 is recruited to a larger complex that peaks near the 5MDa fraction containing XIAP, suggesting Neurl4 and XIAP are both being recruited to the same complex during apoptosis. The red asterisk marks the peak fraction containing Neurl4.

However, what did intrigue us is that Neurl4, much like XIAP, shifts to the 5MDa fraction upon treatment with STS compared to untreated cells. These data suggest that Neurl4 and XIAP are both recruited to the same complex during apoptosis.

Mass spectrometry of the 400kDa XIAP complex

Under normal conditions, XIAP is not monomeric, but rather in an unknown 400kDa complex. This 400kDa complex does not change in response to apoptosis and appears to be a reservoir of XIAP. Using a similar strategy used for identifying the 5MDa complex, we also identified the 400kDa complex by mass spectrometry (Figure 3.10).

Protein	Full name	kDa	MS/MS Area
XIAP	X-linked Inhibitor of Apoptosis	57	1.237E8
TTC19	Tetratricopeptide Repeat Domain 19	42	5.545E6
TXN	Thioredoxin	11	4.822E6
HNRNPU	Heterogeneous Nuclear Ribonucleoprotein U	90	2.012E6
RPL18	60S Ribosomal Protein L18	22	1.980E6
PTBP1	Polypyrimidine Tract Binding Protein 1	57	1.875E6
HLA-DRA	Major Histocompatibility Complex, Class II, DR Alpha	29	1.541E6
HSP90B1	Heat Shock Protein 90kDa Beta (Grp94), Member 1	92	8.217E5

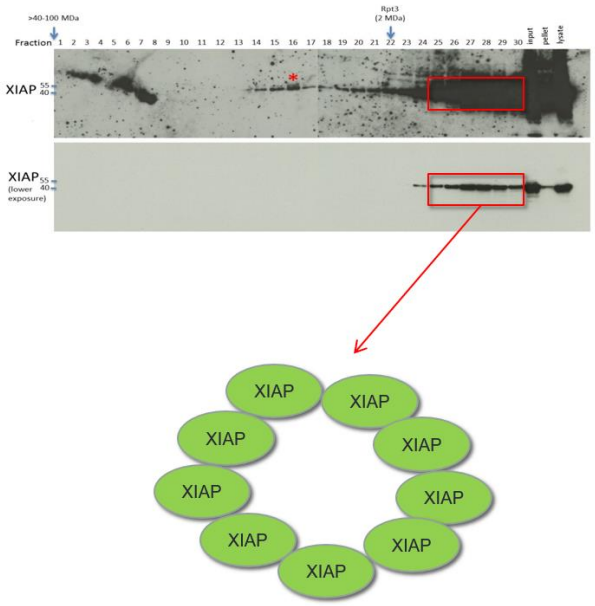

Figure 3.10: Identification of the 400kDa XIAP complex by gel filtration.
Under normal conditions XIAP is found in a 400kDa complex that does not change in response to apoptosis. We identified the proteins in this complex by mass spectrometry and discovered that the complex is a homo-oligomer of XIAP. The list of identified proteins on the left shows that XIAP is more than 20-fold enriched compared to the second-most enriched protein, suggesting that the complex is composed solely of XIAP. The red asterisk indicates the fraction containing the 5MDa complex. The red rectangle indicates the fractions containing the 400kDa XIAP complex. The bottom Western Blot is a lighter exposure of the upper blot.

The mass spectrometry results of the 400kDa complex show that the complex is a homo-oligomer of XIAP, consisting of approximately 8-9 subunits of XIAP. Interestingly, in contrast to the identified proteins of the 5MDa complex, SMAC was not detected in the 400kDa complex. Perhaps this 400kDa complex serves as an inert reservoir of XIAP that prevents XIAP from binding other proteins; only after XIAP is recruited away from this 400kDa is it able to interact with other proteins. This reservoir hypothesis suggests that the cell uses the 400kDa XIAP complex as a mechanism to inhibit XIAP until it is needed.

CHAPTER 4: CHARACTERIZING THE FUNCTIONAL SIGNIFICANCE OF THE COMPLEX IN APOPTOSIS

Testing whether the knockdown of the identified proteins affects apoptosis

Now that we have identified the constituents of the complex, we next want to investigate whether or not they play a functional role in apoptosis. Therefore, we want to study a timepoint in apoptosis where approximately 50% of the cells are apoptotic, so that we can observe if knocking down the identified subunits increases or decreases the number of apoptotic cells. Normally during apoptosis, XIAP is degraded by proapoptotic factors and auto-ubiquitination. ARTS, which is a proapoptotic protein and XIAP antagonist, has been shown to cause the degrading of XIAP after apoptosis induction. Consequently, knockdown of ARTS has shown to delay the degradation of XIAP during apoptosis (Edison et al. 2012). Therefore, we aimed to find a timepoint and concentration of STS that would result in an approximately 50% reduction in XIAP levels (Figure 4.1).

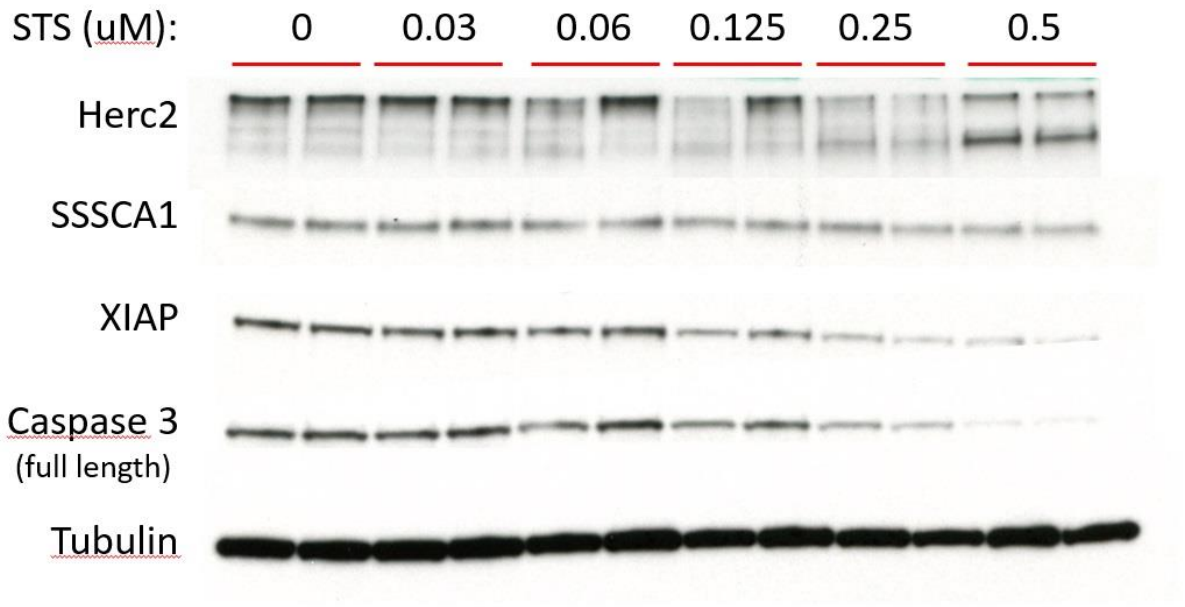

Figure 4.1: Western blot of STS titration in HeLa cells after 5 hours.
HeLa cells were treated with varying amounts of STS for 5 hours. After 5 hours, the cells were collected and analyzed by western blot. Herc2 appears to be cleaved as apoptosis progresses, whereas SSSCA1 does not change. Neurl4 also does not change during apoptosis (data not shown). XIAP levels decrease as apoptosis progresses. Caspase 3 also gets processed into the active form during apoptosis. These data show that cells treated with 0.2M STS for 5 hours have approximately 50% of XIAP remaining, which provides a useful timepoint for testing whether perturbations in the complex's subunits affect apoptosis kinetics.

We chose to use the STS concentration of 0.2uM at 5 hours, since at that timepoint there is an approximately 50% reduction in XIAP levels. Next, wanted to test if knockdowns of the identified subunits would alter the levels of XIAP at this timepoint in apoptosis. To test this, we knocked down each subunit of the complex and looked how it affected the protein levels of the other subunits (Figure 4.2).

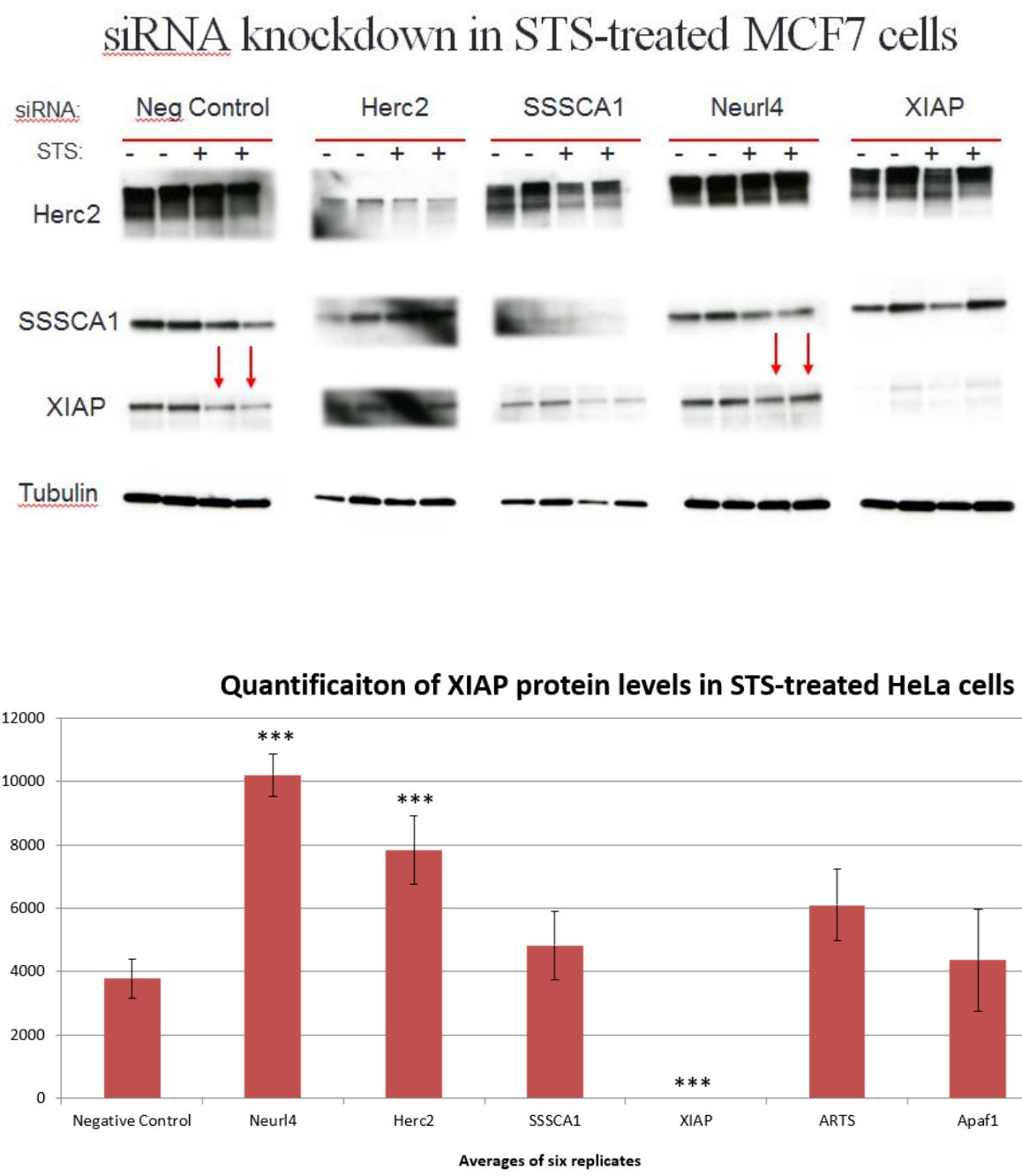

Figure 4.2: Neurl4 knockdown stabilizes XIAP in STS-treated cells.
*siRNA knockdown of the complex's subunits in MCF7 cells with or without 0.5M STS. (a) Westerns of siRNA-treated cells and how the knockdowns affect the protein stability of the other subunits in the STS-treated cells. Neurl4 and Herc2 knockdown stabilizes XIAP during apoptosis compared to the control (red arrows), suggesting that the complex acts to degrade XIAP. (b) The same experiment repeated six times and quantified. Mean and standard error are shown (n = 6). P-values from t-test: ***P<0.0005, relative to the negative control.*

Interestingly, we discovered that the knockdown of Neurl4 stabilizes XIAP during apoptosis, to an extent that is even greater than the XIAP stabilization that is known to occur in the ARTS knockdown line. Finally, counted the number of apoptotic cells for each knockdown to determine if apoptosis was perturbed (Figure 4.3).

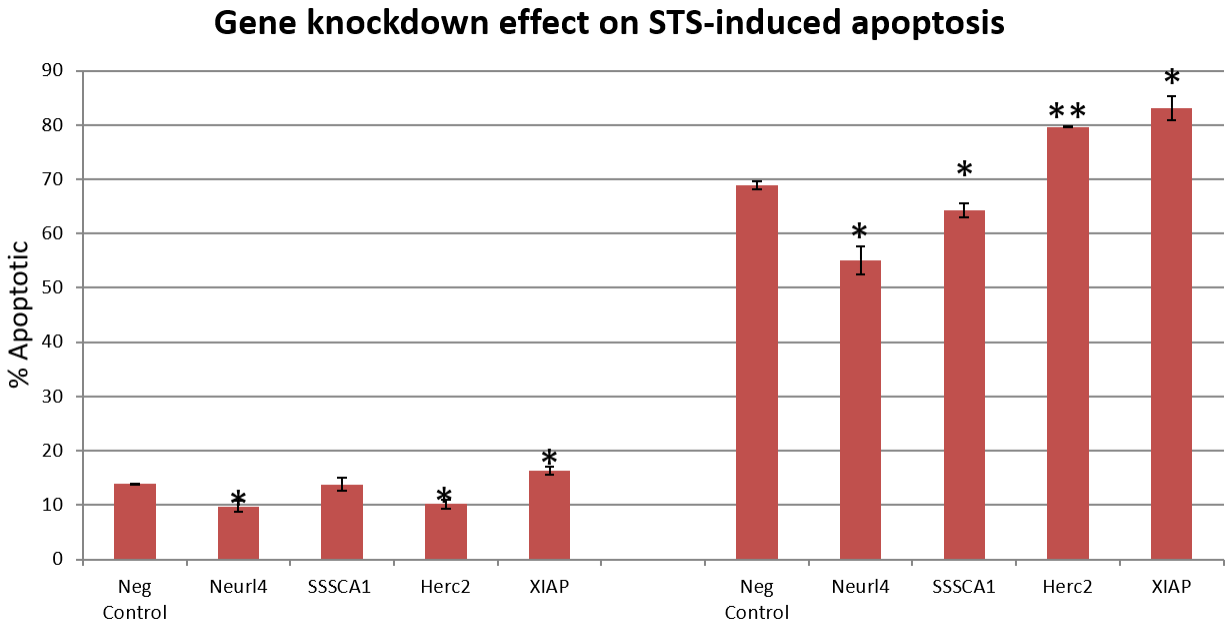

Figure 4.3: Neurl4 knockdown reduces the number of apoptotic cells.
*The complex's subunits were knocked down in HeLa cells by siRNA. The cells were then either untreated or treated with 0.2uM STS for 5 hours and the total number of apoptotic cells was determined by counting apoptotic nuclei. Consistent with Neurl4 knockdown stabilizing XIAP during apoptosis, it also reduced the total number of apoptotic cells by approximately 15%. Intriguingly, Herc2 knockdown increased the total number of apoptotic cells, despite stabilizing XIAP levels. This observation is probably due to the fact that Herc2 is involved in many processes and its knockdown makes cells unhealthy and prone to apoptosis. The knockdown of Neurl4 decreasing the total number of apoptotic cells suggests that this is a proapoptotic complex that acts to degrade XIAP. Mean and standard error are shown (n = 3). P-values from t-test: *P<0.05; **P<0.005, relative to the negative control.*

The knockdown of Neurl4 resulted in a 15% reduction in the number of apoptotic cells, consistent with the observation that Neurl4 knockdown stabilizes XIAP during apoptosis. This result suggests that the complex acts as a pro-apoptotic complex that degrades XIAP during the initiation of apoptosis, thus increasing the propensity of the cells to undergo MOMP and commit

to apoptosis. However, the 15% reduction in apoptosis is quite modest, which encouraged us to repeat these experiments in mouse stem cells, which have been shown to be extremely sensitive to ARTS and XIAP.

Shifting to a mouse model system for *in vivo* experiments

As previously explained, ARTS and XIAP have been shown to have a significant role in the regulation of apoptosis in mouse stem cells. Therefore, we sought out to repeat the human cell line experiments in mouse stem cells, with the hypothesis that these cells would be more sensitive to the knockdown of Neurl4. We chose to use mouse hair follicle stem cells (HFSCs), which are responsible for maintaining hair follicles, and keratinocytes, which are stem cells found at the basal layer of the skin and are the main contributors to the epidermis and wound healing.

Assaying apoptosis in the knockdown keratinocyte lines

To test the effect of the knockdowns on apoptosis in keratinocytes, we used live imaging of caspase activity, combined with image analysis for a high throughput and accurate assay of apoptosis kinetics. We treated the keratinocytes with UV and quantified how many cells became positive for Caspase 3 signal after 15 and 30 hours (Figure 4.4).

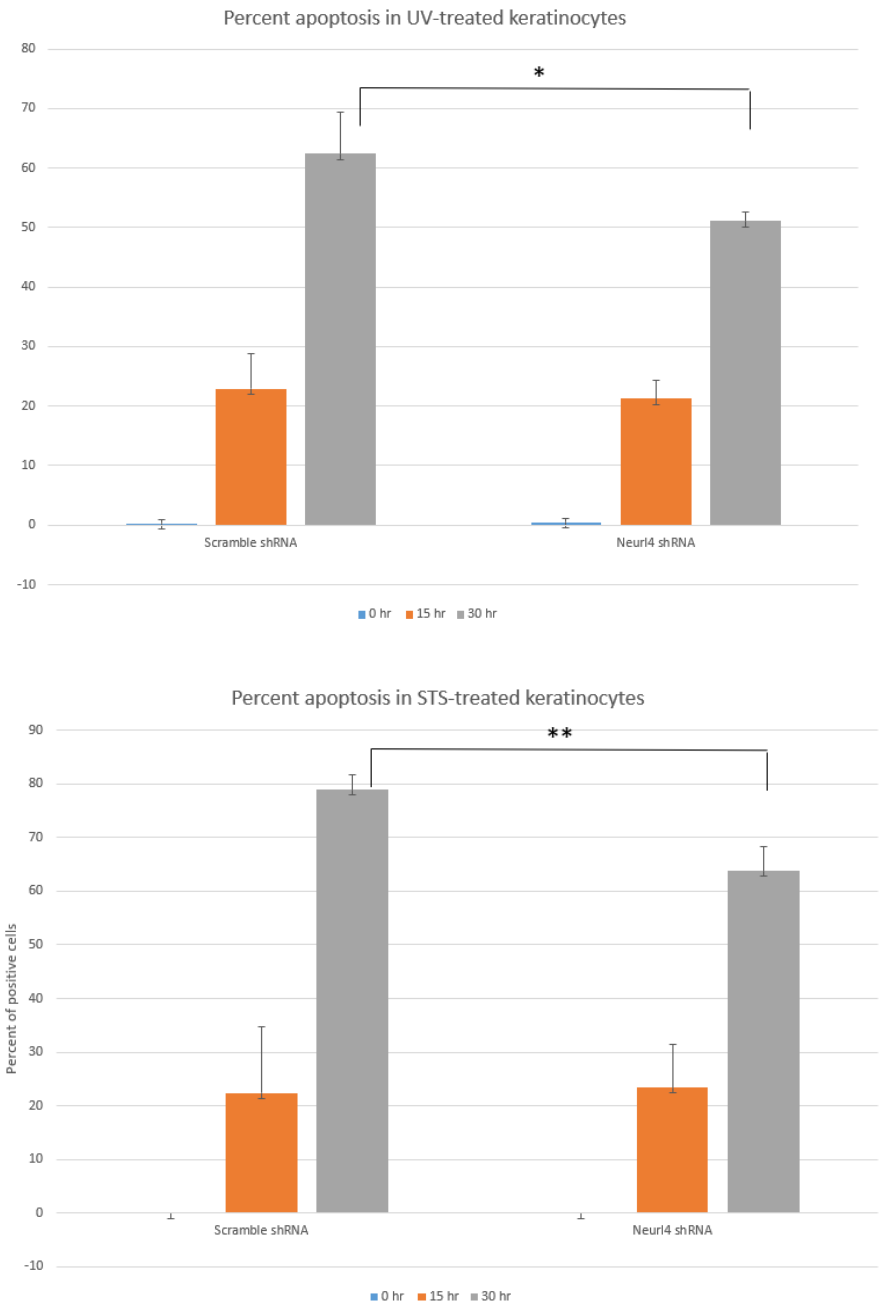

Figure 4.4: Neurl4 knockdown in UV and STS-treated keratinocytes reduces the number of apoptotic cells.
*(Top panel) Keratinocytes were treated with 200uJ of UV followed by quantification of Caspase 3 positive cells after 0, 15 and 30 hours post-exposure. Neurl4 knockdown resulted in an 11% reduction in Caspase 3 positive cells compared to the control. Mean and standard deviation are shown (n = 3). P-values from t-test: *P<0.05. (Bottom panel) Keratinocytes were treated with 1M staurosporine followed by quantification of Caspase 3 positive cells after 0, 15 and 30 hours. Neurl4 knockdown resulted in a 15% reduction in the number of Caspase 3 positive cells compared to the control. These data show that the reduction in apoptosis from Neurl4 knockdown in keratinocytes is similar to the reduction seen in cultured human cell lines. Mean and standard deviation are shown (n = 4). P-values from t-test: **P<0.005.*

Neurl4 knockdown in keratinocytes produced only a modest protection against apoptosis following UV and staurosporine treatment, similar to the results in HeLa cells. One explanation for the mild reduction could be that keratinocytes may not be as sensitive to the levels of ARTS and XIAP, and consequently Neurl4, compared to HFSCs. Another reason why the keratinocytes may not be very sensitive to Neurl4 knockdown could be due to the fact that the keratinocytes used are stable knockdown lines that have acclimated to cell culture. Culturing stem cells has been shown to cause reprogramming that is reminiscent of wound repair (Adam et al., 2015). These reprogrammed cultured stem cells may also have been selected to be resistant to apoptosis after growing in cell culture conditions. To address whether culturing the keratinocytes is causing them to lose their sensitivity to apoptosis, we could knockdown the genes in utero followed by FACS purifying the keratinocytes and performing the apoptosis assay on the freshly purified keratinocytes, before they have a chance to acclimate to cell culture.

Using *Drosophila melanogaster* as a system to study the *in vivo* function of the complex

Drosophila melanogaster is model organism that has been well defined over the years. Because our lab has extensive experience with *Drosophila melanogaster*, we decided to use it as a system to study the biological function of the complex. Specifically, we used the wing imaginal disc of the wandering third instar stage to study the *in vivo* role of the complex in apoptosis. A useful trait of the wing disc is that it is compartmentalized, with specific promoters driving expression in well-defined areas (Figure 3.11).

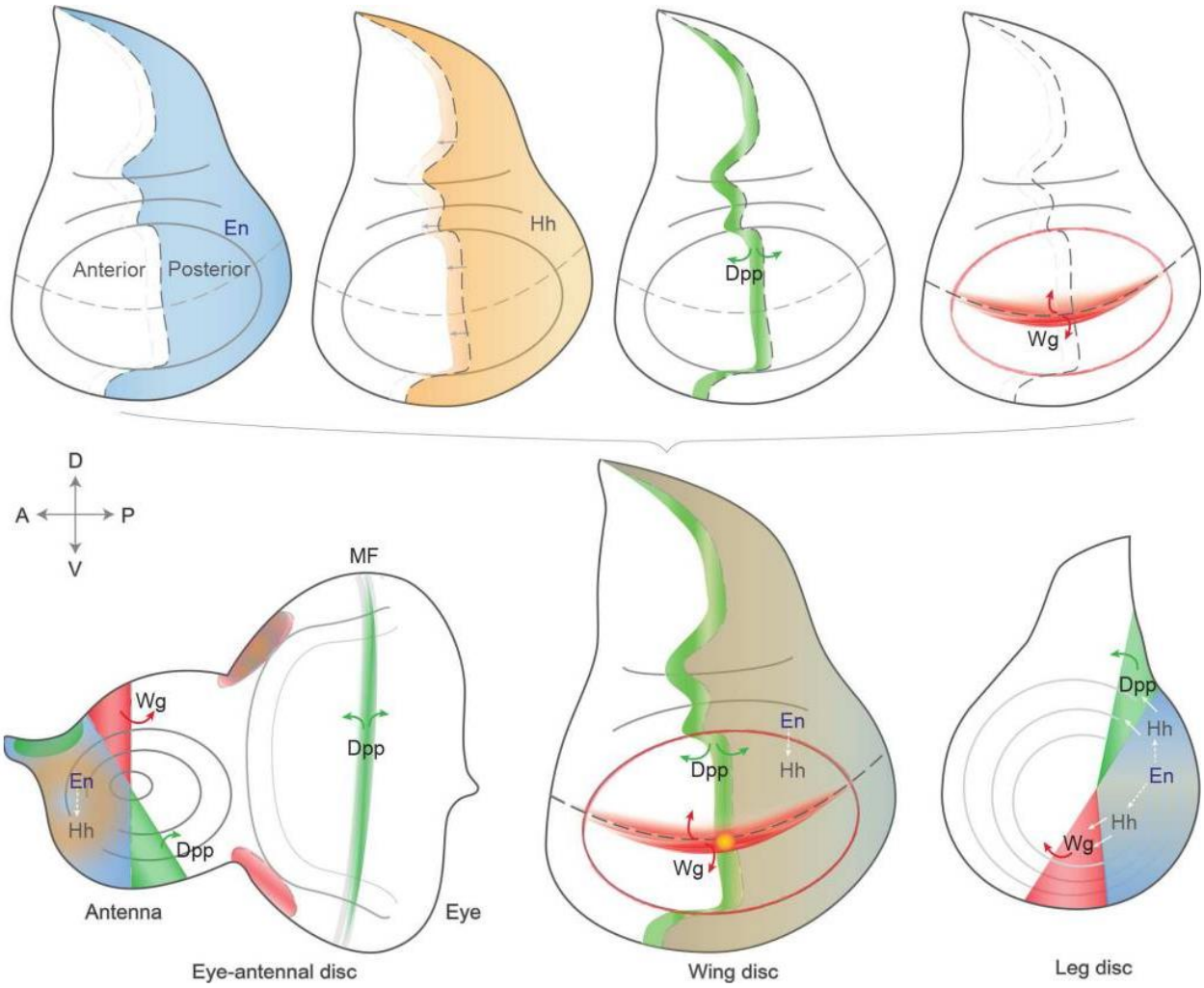

Figure 3.11: The expression patterns in the imaginal discs of Drosophila melanogaster. The larva of Drosophila melanogaster contain imaginal discs that give rise to specific structures in the adult fly. A useful trait of the imaginal discs is the compartmentalized expression of specific transcription factors, which can be used to either overexpress or knockdown genes in their corresponding compartment and compared to the unaffected, wild-type section of the same imaginal disc (Beira & Paro, 2016).

Using Engrailed-GAL4 coupled with UAS-EP or UAS-RNAi, we are able to either overexpress or knockdown genes, respectively, in the posterior compartment of the wing disc. We treated the wing discs with staurosporine to induce apoptosis and visualized the apoptotic cells by immunofluorescence using Hoechst for total DNA, anti-γ-H2Av to label phosphorylated histone H2Av (a marker that indicates DNA damage), and anti-Caspase 3 (Figure 3.12).

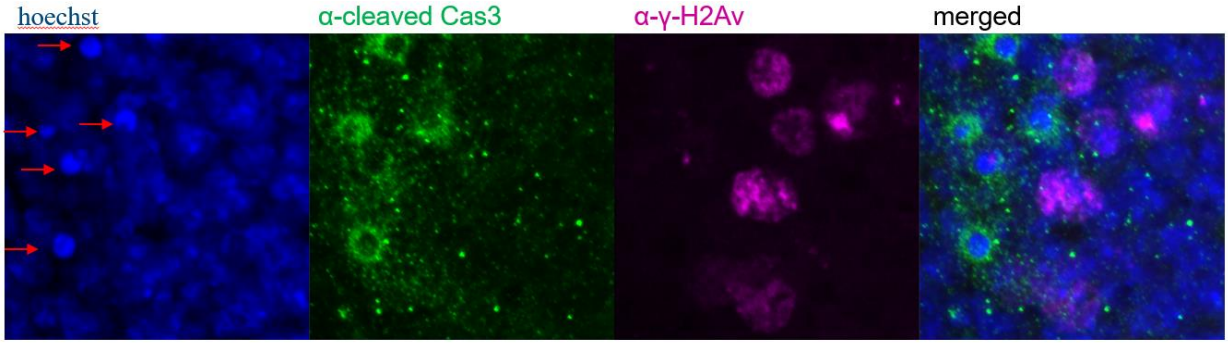

Figure 3.12: Optimizing apoptotic markers in staurosporine-treated wing discs of Drosophila melanogaster.
Imaginal wing discs from wild-type third instar larva were treated in-situ with 1M staurosporine for 4 hours and imaged by immunofluorescence. A late phenotypic marker of apoptosis is the condensation of DNA into foci (red arrows). However, before the DNA can be condensed, it is first cleaved, primarily by the protein CAD. The cleavage of the DNA is marked by the γ phosphorylation of the histone H2Av (magenta). Cleaved Caspase 3, which is the active form, is another indicator of apoptosis (green). Interestingly, we observed that γ-H2Av marks an earlier apoptotic timepoint than cleaved Caspase 3, which labels apoptotic cells the at the late timepoint of DNA condensation.

The staining of the wing discs revealed that DNA condensation and active Caspase 3 (DrICE and Dcp-1 in *Drosophila melanogaster*) signal marked similar timepoints, whereas γ-H2Av labeled cells at an earlier timepoint in apoptosis. The observation that γ-H2Av labels apoptotic cells before active Caspase 3 is counter-intuitive because active caspases are required for CAD's activation and subsequent DNA cleavage (Tang & Kidd, 1998). A possible explanation for why γ-H2Av labels cells before active Caspase 3 is that the anti-cleaved Caspase 3 antibody also labels the cleaved substrates of Caspase 3, and only after a sufficient amount of cleaved substrate accumulates is there enough signal for detection, which might occur later than the γ phosphorylation of H2Av. These data show that the γ-H2Av and cleaved Caspase 3 antibodies can be used to label cells at different timepoints in apoptosis.

After validating antibodies to label apoptosis in the wing disc, we next needed to optimize the timing of apoptosis in the wing disc so that some, but not all cells have undergone apoptosis. To find a suitable timepoint, we treated wing discs *in-situ* with staurosporine for various timepoints;

Engrailed-GAL4 UAS-DsRed2 was used to label the compartment of the wing disc (posterior) that expresses Engrailed in red (Figure 3.13).

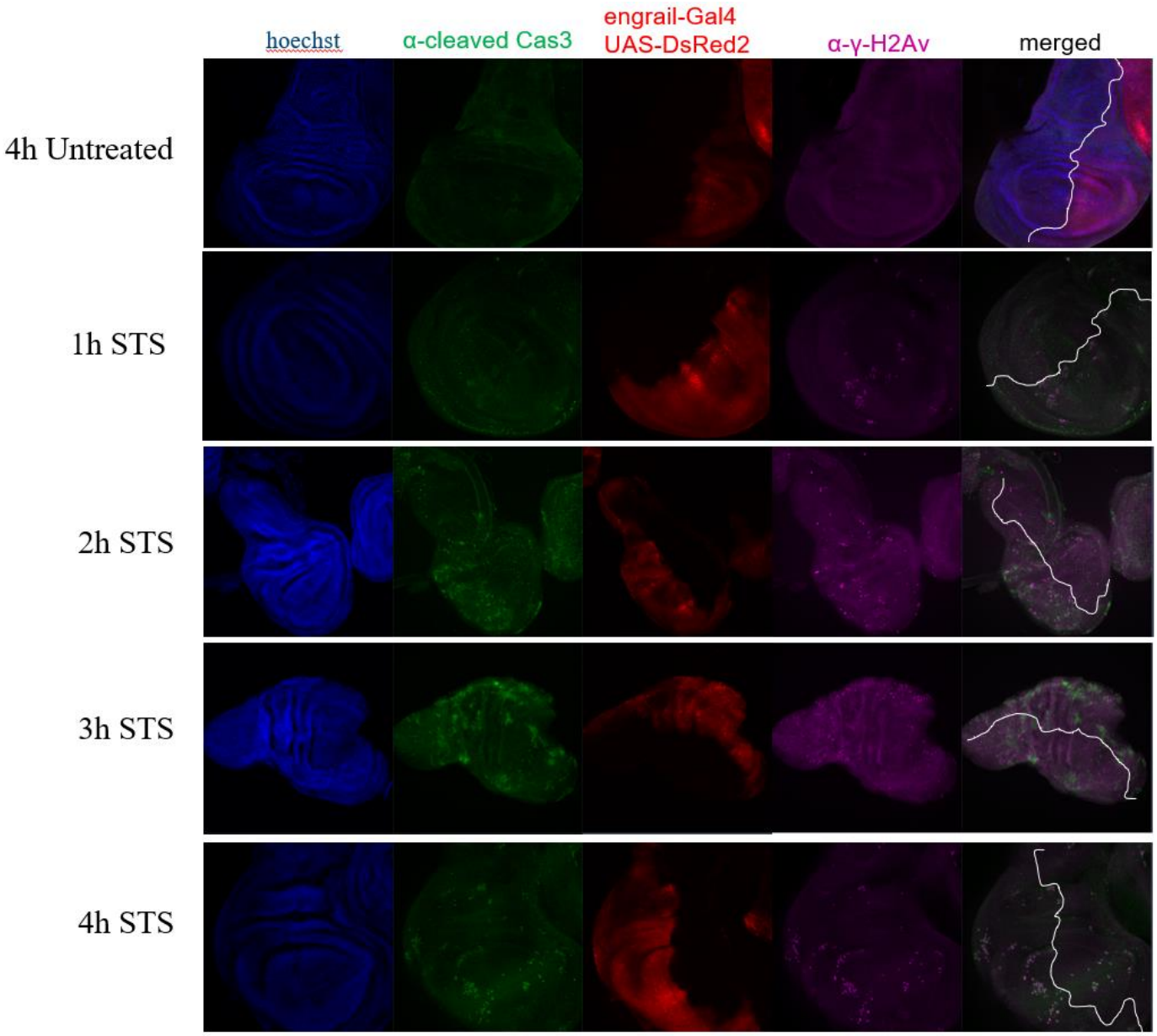

Figure 3.11: Wing discs treated with staurosporine for various timepoints.

Third instar imaginal wing discs were treated in-situ with 1M staurosporine for 1hr, 2hr, 3hr and 4 hrs and imaged by immunofluorescence. Although all staurosporine timepoints resulted in inducing apoptosis, the three hour timepoint produced the most consistent results. Blue = Hoechst; Green = anti-Cleaved Caspase 3; Red = Engrailed-GAL UAS-DsRed2; Magenta = anti-γ-H2Av; White line = the anterior/posterior interface.

The above data show that all timepoints of staurosporine treatment resulted in apoptotic cells compared to the untreated control. However, the three-hour treatment of staurosporine resulted in a more consistent number of apoptotic cells compared to the other timepoints, which had large variation in the number of apoptotic cells (data not shown).

To study if the complex affects apoptosis in the wing discs, we crossed flies to either overexpress or knockdown Neurl4 (bluestreak or blue in the fly) under the control of Engrailed so we could compare to results to the unaffected anterior compartment of the wing disc as an internal control (Figure 3.16).

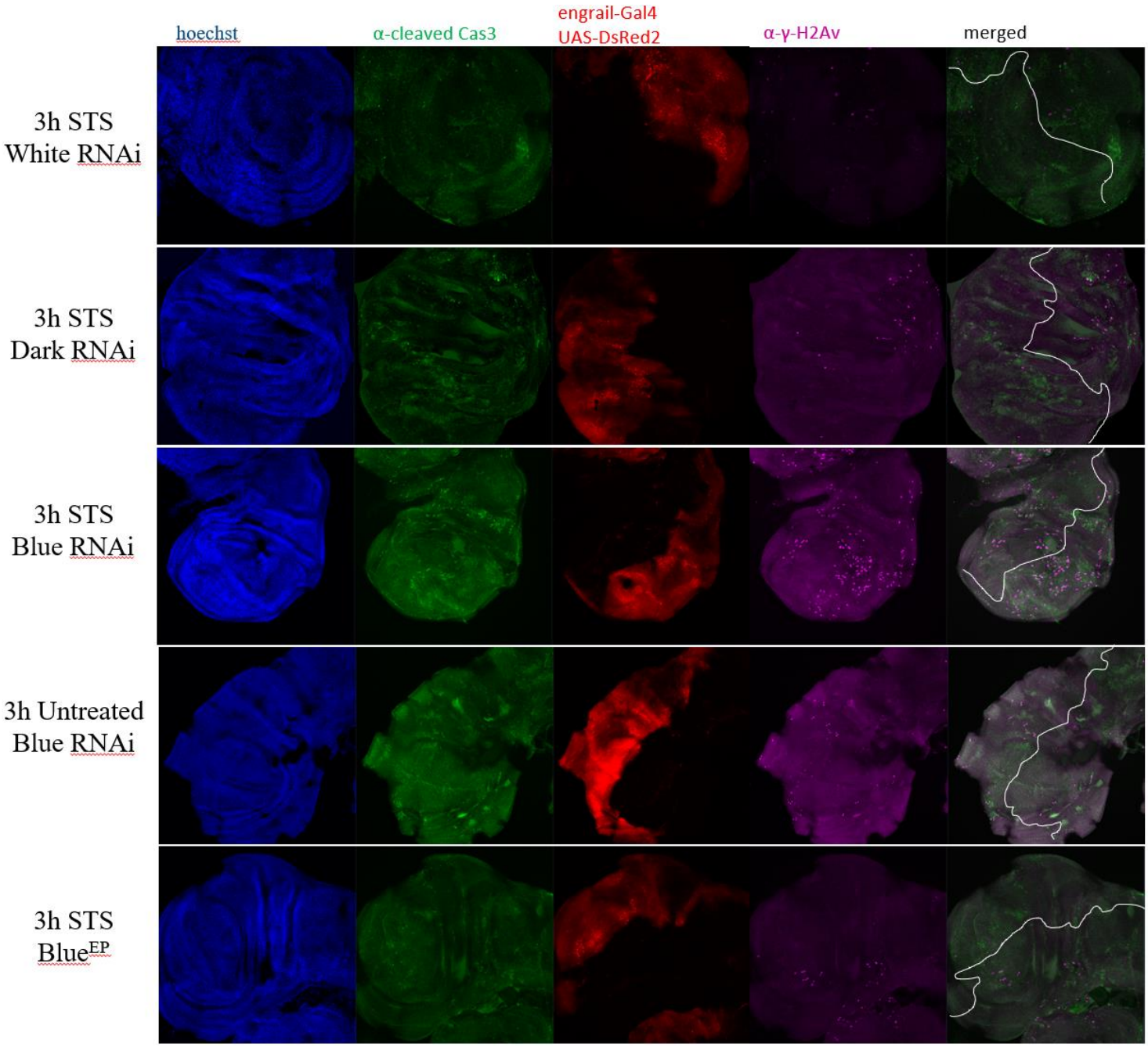

Figure 3.11: The effect of staurosporine on wing discs that are either knocked down for or overexpressing Neurl4.
Third instar wing discs were treated in-situ with 1M staurosporine for 3 hours and imaged by immunofluorescence. The RNAi and overexpression is under the control of the Engrailed-Gal4 UAS system. The knockdown and overexpression of Neurl4 (Blue in the fly) was localized to the posterior (labeled in red) compartment of the wing disc. The anterior compartment of the wing disc can be used as a wild-type internal control. After treatment with staurosporine, the posterior compartment had higher numbers of apoptotic cells compared to the anterior compartment in all cases. Gal4 overexpression has been observed to induce cytotoxicity and primes the cells for apoptosis compared to the wild-type anterior compartment, which lacks Gal4 overexpression. Therefore, because Gal4 produces a high apoptosis background, this system is not suitable for studying how the complex affects apoptosis. The white gene served as the control for Gal4. Dark RNAi (Apaf1 in mammals) was used as a control for the ability to inhibit apoptosis in this system. This experiment was repeated several times with the same results (data not shown).

Neurl4 (bluestreak or blue in *Drosophila)* was the only member of the complex that had flies available for RNAi and overexpression. The white gene was used as a control for Gal4 overexpression and Dark (Apaf1 in mammals) knockdown was used as a control for the ability to inhibit staurosporine-induced apoptosis in this system. Dark has been well characterized in the fly and has been shown to be crucial for proper apoptosis, so its knockdown inhibiting apoptosis in this system was not surprising (Rodriguez et al., 1999). However, what immediately stood out to us was the fact that there were higher numbers of apoptotic cells in the Engrailed Gal4 posterior compartment in all of the other conditions. Looking through the literature, we discovered that Gal4 overexpression has been observed to cause cytotoxicity (Kramer & Staveley, 2003). After repeating this experiment several times with the same results, we concluded that the Gal4 overexpression system is not suitable for studying how the complex affects apoptosis, since Gal4 overexpression is creating a high apoptosis background. An alternative approach would be to drive the knockdown and overexpression of Neurl4 using a different driver, such as tubulin. The appeal of using *Drosophila* to test the complex *in vivo* was that the tools and resources to do the experiments were readily available. However, since switching drivers would require us to create new fly lines from scratch, we decided it would be best to focus our efforts on mammalian cells, since that is where we have established the complex so far.

CHAPTER 5. DISCUSSION

We sought out to understand what accounts for the variability of apoptosis kinetics between cells. Since apoptosis becomes robust and predictable following MOMP, it was obvious to us that the cause of the variance must be very early in apoptosis, upstream of MOMP. Looking for changes in canonical apoptosis proteins at early timepoints, we discovered that XIAP is recruited to a 5MDa complex as early as 30 minutes after induction of apoptosis, and that this recruitment of XIAP to the complex is dependent on ARTS. We identified the subunits of the complex being Herc2, Neurl4, SSSCA1 and XIAP. Furthermore, we showed that the complex acts to degrade XIAP and priming the cells to die, because when Neurl4 is knocked down, XIAP becomes stabilized during apoptosis, resulting in fewer apoptotic cells (Figure 5.1).

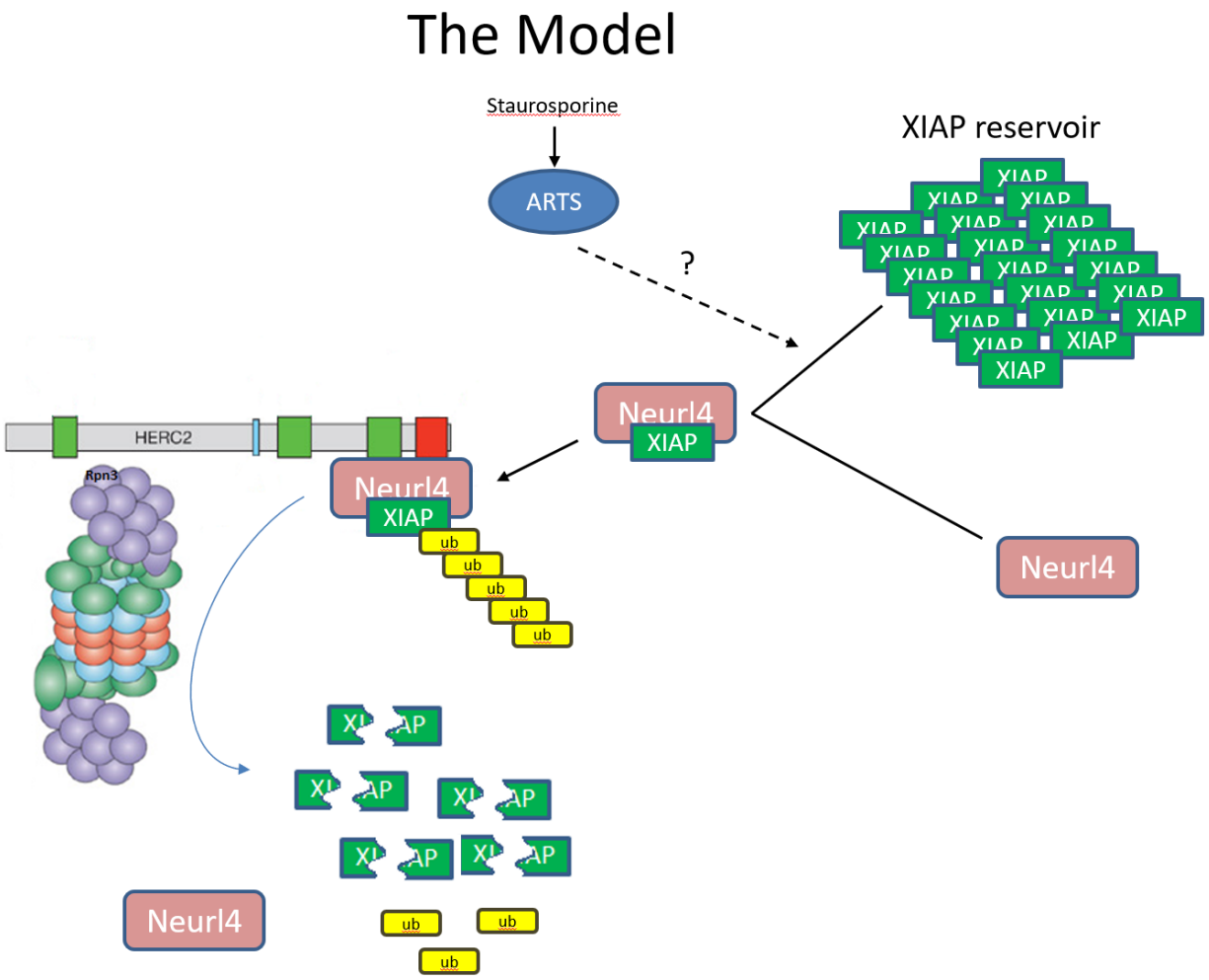

Figure 5.1: The postulated model of how the complex recruits and degrades XIAP. Under normal conditions XIAP is found in an inert 400kDa complex. However, upon apoptosis induction, ARTS recruits XIAP to the 5MDa complex, where XIAP is ubiquitinated and degraded, thus priming cells to die.

However, after only seeing a 15% reduction in apoptosis in the human cell lines, we hypothesized that we would observe a more pronounced effect in mouse stem cells, since previous studies have shown XIAP and ARTS playing a pivotal role in regular apoptosis in these cells. Disappointingly, we saw similar results for the mouse stem cells.

A likely explanation for why the results were similar is that the process of cells adapting to the cell culture environment reprograms the cells, making them more resistant to apoptosis

compared to their *in vivo* counterparts. There is a recent study supporting this idea, which shows that stem cells that are taken out of their *in vivo* environment and put into cell culture immediately undergo reprogramming that is very reminiscent of a wound healing profile (Figure 5.2; (Adam et al., 2015)).

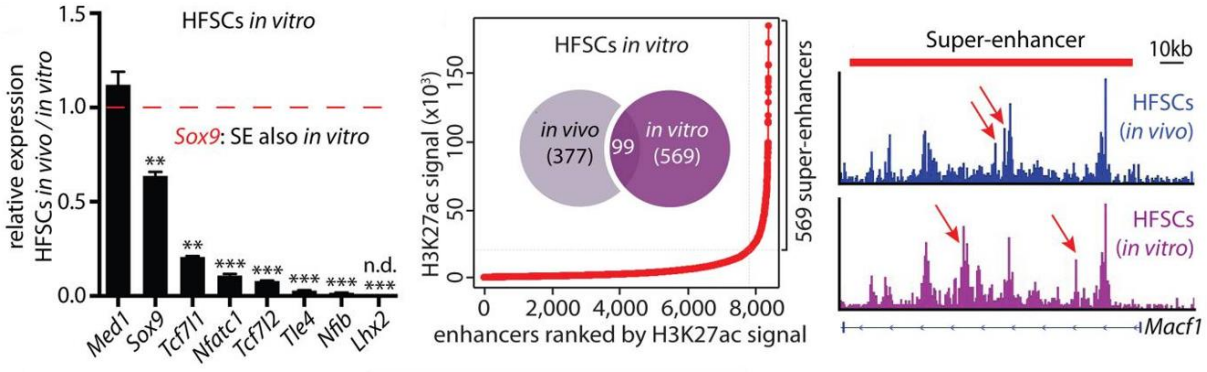

Figure 5.2: Stem cells undergo extensive reprogramming when removed from their in-vivo niche and put into culture.
The left panel shows that many signature stem cell transcription factors are down-regulated when the stem cells are put into culture. Many wound repair genes, such as Macf1, are also upregulated in cultured stem cells. If the cell culture environment is harsh and reminiscent of a wound, then perhaps this could explain why cells that survive in culture are resistant to apoptosis compared to their in-vivo counterparts (Adam et al., 2015).

In addition, it has been shown that mouse HFSCs are extremely susceptible to apoptotic stimuli when they are freshly sorted and immediately assays before they are allowed to undergo reprogramming in a cell culture environment (Figure 5.2).

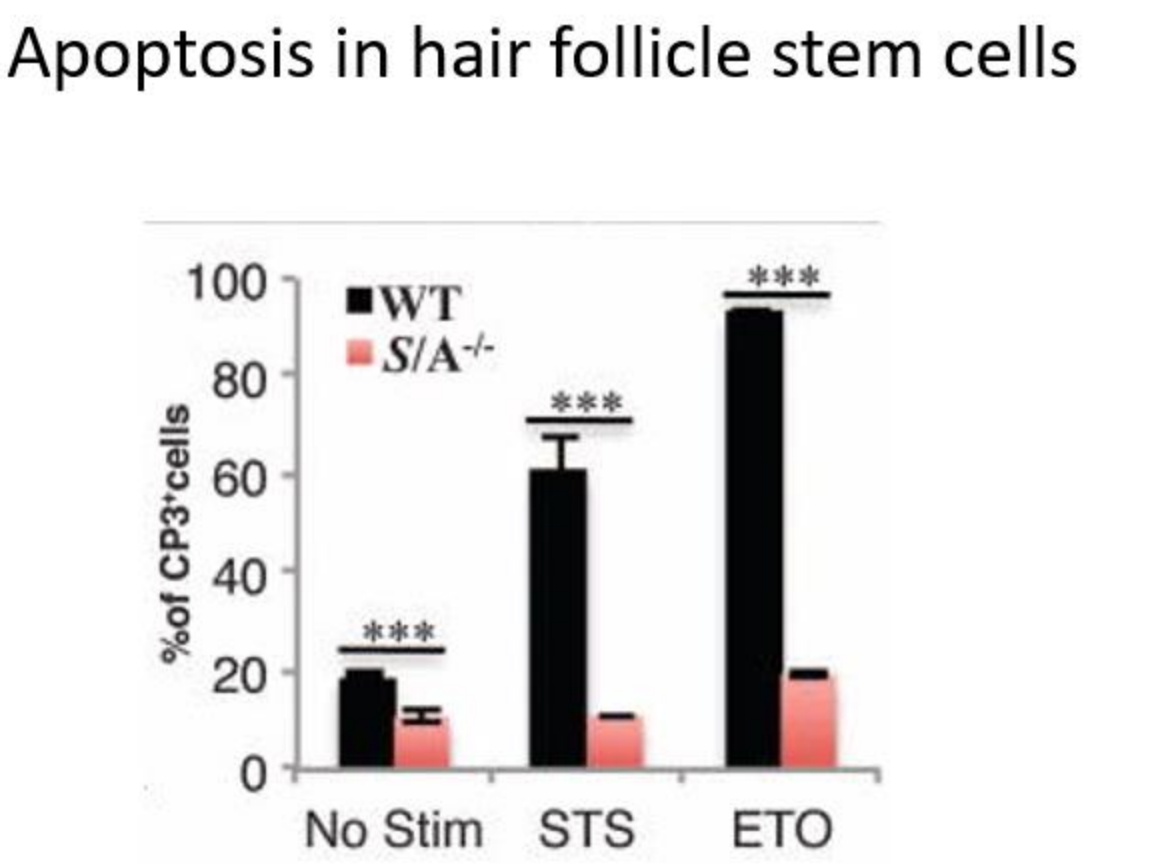

Figure 5.2: Apoptosis in freshly sorted HFSCs is dependent on ARTS.
Mouse HFSCs freshly sorted and immediately treated with STS or ETO and quantified for Caspase 3 positive cells by flow cytometry. Unlike most cultured cell lines, apoptosis in HFSCs is extremely sensitive the knockout of ARTS. This study highlights the particular importance of ARTS in stem cell homeostasis (Fuchs et al., 2013).

Looking forward, the best approach to studying apoptosis in stem cells appears to be *in vivo*, since the cells seem to lose their sensitivity to apoptosis after acclimating to cell culture. Fortunately, there are myriad methods for studying apoptosis in an *in vivo* model system. One way is to do all of the assays with freshly sorted stem cells before they have time to reprogram. Wound healing of the skin is another powerful model system for studying stem cell apoptosis *in vivo*. Nonetheless, the discovery of this novel 5MDa complex is exciting. The discovery has implicated new players in apoptosis, it gives insight into the decision-making mechanism cells

undergo before committing to cell death, and provides potential for new therapeutics to be developed to modulate apoptosis.

CHAPTER 6. BIBLIOGRAPHY

Adam, R. C., Yang, H., Rockowitz, S., Larsen, S. B., Nikolova, M., Oristian, D. S., . . . Fuchs, E. (2015). Pioneer factors govern super-enhancer dynamics in stem cell plasticity and lineage choice. *Nature, 521*(7552), 366-370. doi:10.1038/nature14289

Beira, J. V., & Paro, R. (2016). The legacy of Drosophila imaginal discs. *Chromosoma, 125*(4), 573-592. doi:10.1007/s00412-016-0595-4

Beronja, S., Livshits, G., Williams, S., & Fuchs, E. (2010). Rapid functional dissection of genetic networks via tissue-specific transduction and RNAi in mouse embryos. *Nature medicine, 16*(7), 821-827. doi:10.1038/nm.2167

Boldin, M P; Goncharov T M, Goltsev Y V, Wallach D (1996). Involvement of MACH, a novel MORT1/FADD-interacting protease, in Fas/APO-1- and TNF receptor-induced cell death". *Cell* **85** (6): 803–15.

Bornstein B, Gottfried Y, Edison N, Shekhtman A, Lev T, Glaser F, Larisch S (2011). ARTS binds to a distinct domain in XIAP-BIR3 and promotes apoptosis by a mechanism that is different from other IAP-antagonists. *Apoptosis* **16**(9):869-81.

Chinnaiyan AM, O'Rourke K, Lane BR, Dixit VM (1997). Interaction of CED-4 with CED-3 and CED-9: a molecular framework for cell death. *Science* **275**: 1122–1126.

Deveraux QL, Takahashi R, Salvesen GS, Reed JC. (1997) X-linked IAP is a direct inhibitor of cell-death proteases. *Nature* **388**(6639):300-4.

Du C, Fang M, Li Y, Li L, Wang X (2000). Smac, a mitochondrial protein that promotes cytochrome c-dependent caspase activation by eliminating IAP inhibition. *Cell* **102**(1): 33-42.

Edison N, Zuri D, Maniv I, Bornstein B, Lev T, Gottfried Y, Kemeny S, Garcia-Fernandez M, Kagan J, Larisch S (2012). The IAP-antagonist ARTS initiates caspase activation upstream of cytochrome C and SMAC/Diablo. *Cell Death Differ* **19**(2):356-68.

Farrow SN, White JH, Martinou I, Raven T, Pun KT, Grinham CJ, Martinou JC, Brown R. (1995) Cloning of a bcl-2 homologue by interaction with adenovirus E1B 19K. *Nature* **374**(6524): 731-3.

Fernandes-Alnemri T, Litwack G, Alnemri ES (1994). CPP32, a novel human apoptotic protein with homology to Caenorhabditis elegans cell death protein Ced-3 and mammalian interleukin-1 beta-converting enzyme. *J. Biol. Chem.* **269** (49): 30761–4.

Fu J, Jin Y, Arend LJ. (2003) Smac3, a novel Smac/DIABLO splicing variant, attenuates the stability and apoptosis-inhibiting activity of X-linked inhibitor of apoptosis protein. *J Biol Chem* **278**: 52660–52672.

Fuchs Y, Brown S, Gorenc T, Rodriguez J, Fuchs E, Steller H (2013). Sept4/ARTS regulates stem cell apoptosis and skin regeneration. *Science* **341**(6143):286-9.

Fuchs, Y., & Steller, H. (2011). Programmed cell death in animal development and disease. *Cell, 147*(4), 742-758. doi:10.1016/j.cell.2011.10.033

García-Fernández, M., Kissel, H., Brown, S., Gorenc, T., Schile, A. J., Rafii, S., . . . Steller, H. (2010). Sept4/ARTS is required for stem cell apoptosis and tumor suppression. *Genes & Development, 24*(20), 2282-2293. doi:10.1101/gad.1970110

Goldstein JC, Kluck RM, Green DR (2000). A single cell analysis of apoptosis. Ordering the apoptotic phenotype. *Ann N Y Acad Sci* **926**:132-41.

Gottfried Y, Rotem A, Lotan R, Steller H, Larisch S (2004). The mitochondrial ARTS protein promotes apoptosis through targeting XIAP. *EMBO J* **23**(7):1627-35.

Goldstein JC, Muñoz-Pinedo C, Ricci JE, Adams SR, Kelekar A, Schuler M, Tsien RY, Green DR (2005). Cytochrome c is released in a single step during apoptosis. *Cell Death Differ* **12**(5):453-62.

Hill MM, Adrain C, Duriez PJ, Creagh EM, Martin SJ. Analysis of the composition, assembly kinetics and activity of native Apaf-1 apoptosomes. *Embo J* **23**: 2134–45.

Hsu H, Xiong J, Goeddel DV (1995). The TNF receptor 1-associated protein TRADD signals cell death and NF-kappa B activation. *Cell* (1995) **81** (4): 495-504.

Jacobson, M. D., Weil, M., & Raff, M. C. (1997). Programmed cell death in animal development. *Cell, 88*(3), 347-354.

Joza N, Susin SA, Daugas E, Stanford WL, Cho SK, Li CY, Sasaki T, Elia AJ, Cheng HY, Ravagnan L, Ferri KF, Zamzami N, Wakeham A, Hakem R, Yoshida H, Kong YY, Mak TW, Zúñiga-Pflücker JC, Kroemer G, Penninger JM (2001). Essential role of the mitochondrial apoptosis-inducing factor in programmed cell death. *Nature* **410**(6828):549-54.

Joazeiro CA, Weissman AM. (2000) RING finger proteins: mediators of ubiquitin ligase activity. *Cell* **102**(5):549-52.

Kramer, J. M., & Staveley, B. E. (2003). GAL4 causes developmental defects and apoptosis when expressed in the developing eye of Drosophila melanogaster. *Genet Mol Res, 2*(1), 43-47.

Kischkel FC, Hellbardt S, Behrmann I, Germer M, Pawlita M, Krammer PH and Peter ME. (1995) Cytotoxicity-dependent APO-1 (Fas/CD95)-associated proteins form a death-inducing signaling complex (DISC) with the receptor. *EMBO J* **14**: 5579–5588.

Larisch S, Yi Y, Lotan R, Kerner H, Eimerl S, Tony Parks W, Gottfried Y, Birkey Reffey S, de Caestecker MP, Danielpour D, Book-Melamed N, Timberg R, Duckett CS, Lechleider RJ, Steller H, Orly J, Kim SJ, Roberts AB (2000). A novel mitochondrial septin-like protein, ARTS, mediates apoptosis dependent on its P-loop motif. *Nature Cell Biol* **2**(12):915-21.

Luo X, Budihardjo I, Zou H, Slaughter C, Wang X (1998). Bid, a Bcl2 Interacting Protein, Mediates Cytochrome c Release from Mitochondria in Response to Activation of Cell Surface Death Receptors. *Cell* **94**(4): 481-490.

Martins LM, Iaccarino I, Tenev T, Gschmeissner S, Totty NF, Lemoine NR, Savopoulos J, Gray CW, Creasy CL, Dingwall C, Downward J (2001). The serine protease Omi/HtrA2 regulates apoptosis by binding XIAP through a reaper-like motif. *J Biol Chem* **277**(1):439-44.

Nakano K, Vousden KH (2001). PUMA, a novel proapoptotic gene, is induced by p53. *Mol. Cell* **7** (3): 683–94.

Nicholson DW, Ali A, Thornberry NA, Vaillancourt JP, Ding CK, Gallant M, Gareau Y, Griffin PR, Labelle M, Lazebnik YA (1995). Identification and inhibition of the ICE/CED-3 protease necessary for mammalian apoptosis, *Nature* **376** (6535): 37–43.

Oda, E; Ohki R, Murasawa H, Nemoto J, Shibue T, Yamashita T, Tokino T, Taniguchi T, Tanaka N (2000). Noxa, a BH3-only member of the Bcl-2 family and candidate mediator of p53-induced apoptosis. *Science* **288**(5468): 1053–8.

Oltvai ZN, Milliman CL, Korsmeyer SJ (1993). Bcl-2 heterodimerizes *in vivo* with a conserved homolog, Bax, that accelerates programmed cell death. *Cell* **74**(4): 609-19.

Rodriguez J, Lazebnik Y (1999). Caspase-9 and APAF-1 form an active holoenzyme. *Genes Dev* **13**(24):3179-84.

Rodriguez, A., Oliver, H., Zou, H., Chen, P., Wang, X., & Abrams, J. M. (1999). Dark is a Drosophila homologue of Apaf-1/CED-4 and functions in an evolutionarily conserved death pathway. *Nat Cell Biol, 1*(5), 272-279. doi:10.1038/12984

Schile AJ, García-Fernández M, Steller H. (2008) Regulation of apoptosis by XIAP ubiquitin-ligase activity. *Genes Dev* **22**(16):2256-66.

Seshagiri S, Miller L. (1997**)** *Caenorhabditis elegans* CED-4 stimulates CED-3 processing and CED-3-induced apoptosis. *Curr Biol* **7**:455–460.

Soteriou, D., Kostic, L., Sedov, E., Yosefzon, Y., Steller, H., & Fuchs, Y. (2016). Isolating Hair Follicle Stem Cells and Epidermal Keratinocytes from Dorsal Mouse Skin. *Journal of Visualized Experiments : JoVE*(110), 53931. doi:10.3791/53931

Spencer, S. L., & Sorger, P. K. (2011). Measuring and Modeling Apoptosis in Single Cells. *Cell, 144*(6), 926-939. doi:10.1016/j.cell.2011.03.002

Srinivasula SM, Ahmad M, Fernandes-Alnemri T, Litwack G, Alnemri ES. (1996). Molecular ordering of the Fas-apoptotic pathway: the Fas/APO-1 protease Mch5 is a CrmA-inhibitable protease that activates multiple Ced-3/ICE-like cysteine proteases. *Proc. Natl. Acad. Sci. U.S.A.* **93** (25): 14486–91.

Tang, D., & Kidd, V. J. (1998). Cleavage of DFF-45/ICAD by multiple caspases is essential for its function during apoptosis. *J Biol Chem, 273*(44), 28549-28552.

Verhagen AM, Ekert PG, Pakusch M, Silke J, Connolly LM, Reid GE, Moritz RL, Simpson RJ, Vaux DL (2000). Identification of DIABLO, a mammalian protein that promotes apoptosis by binding to and antagonizing IAP proteins. *Cell* **102**(1): 43-53.

Xuan J, Horvitz HR (1992). The *Caenorhabditis elegans* cell death gene *ced-4* encodes a novel protein and is expressed during the period of extensive programmed cell death. *Development* **116**(2):309-20.

Zou H, Henzel WJ, Liu X, Lutschg A, Wang X. (1997) Apaf-1, a human protein homologous to *C. elegans* CED-4, participates in cytochrome c-dependent activation of caspase 3. *Cell* **90** (3): 405-13.